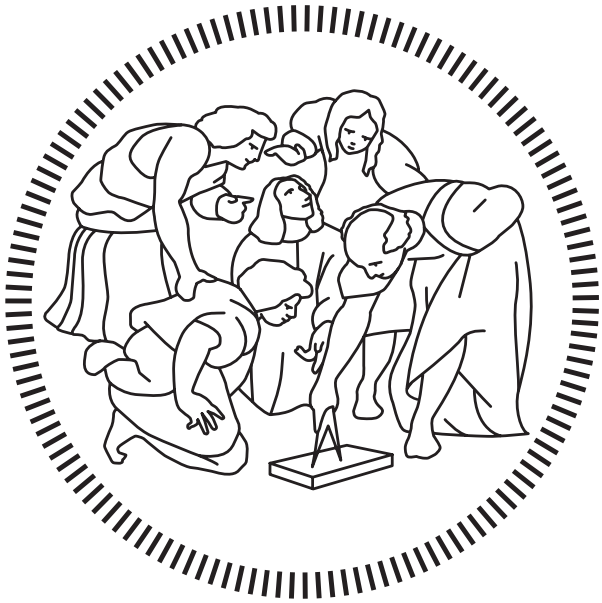

POLITECNICO DI MILANO

School of Industrial and Information Engineering
Department of Aerospace Science and Technology
MSC in Aeronautical Engineering

ANALYSIS AND DESIGN OF A 20MW TWO-BLADED WIND TURBINE

Author:
Samuele Foresti
921098

Supervisor:
Prof. Alessandro Croce

Academic Year 2019 – 2020

Ringraziamenti

Vorrei innanzitutto ringraziare il mio relatore, Professore Alessandro Croce, per aver suscitato in me l'interesse per l'energia eolica e per avermi dato l'opportunità di intraprendere questo lavoro di tesi. Un doveroso ringraziamento anche a Luca Sartori per i consigli tecnici nei primi mesi di lavoro e per avermi fornito le basi per poter utilizzare il software Cp-Max. Un grande grazie anche a Federico, collega in questi mesi di tesi, con cui ho condiviso molto consigli e suggerimenti tecnici, ma anche chiacchierate di piacere e di supporto morale.

Un ringraziamento speciale a Ilaria, per i preziosi momenti trascorsi insieme in questi anni e per avermi trasmesso la forza e il coraggio per non arrendermi mai. Un enorme grazie anche ai suoi genitori, per essere stati una seconda famiglia e per il concreto supporto tecnico.

Un ringraziamento agli amici del Poli. Grazie a tutte le persone che ho avuto modo di conoscere in questa esperienza universitaria e con i quali ho condiviso numerose ore in aula, molti litri di caffè, intense ore di studio, e infiniti viaggi in treno. Soprattutto grazie per quelle amicizie che non si sono limitate all'ambito accademico, ma che hanno proseguito fuori dalle aule, alimentando le nostre comuni passioni e la voglia di condividere e trascorre tempo insieme.

Un ringraziamento alle fantastiche persone incontrate durante l'esperienza vissuta in Colombia, in particolare a Lorenzo e Carolina, che da semplici coinquilini sono diventati poi grandi amici e compagni di avventure; alle amiche di sempre, Annapaola, Carolina e Michela, che ho la fortuna di conoscere letteralmente da tutta la vita e che nonostante le diverse strade intraprese sono e saranno sempre un porto sicuro; agli amici della compagnia, per le indimenticabili vacanze insieme a bordo della Delta e per il loro travolgente e immancabile spirito positivo; agli amici di San Fermo, punto cardine per il mio percorso di crescita personale e umana; all'amico Andrea, sempre pronto per i viaggi più folli che si possano immaginare; agli amici di SirCharlesLeeptonHaisTee, gli amici "grandi", con cui ho trascorso molte avventure e dai quali ho sempre qualcosa da imparare; agli amici dello sport, in particolare Xaver e Manu, con i quali ho percorso moltissima strada, scoperto posti meravigliosi, condiviso preziosi silenzi, e attraverso la fatica e il sudore ho appreso valori come l'impegno, la costanza e la correttezza; agli amici di SoBritish, con i quali nonostante ci si veda sporadicamente è sempre bello ritrovarsi e ricordare le belle avventure del Liceo.

Infine un ringraziamento immenso alla mia famiglia per avermi dato l'opportunità di affrontare questo prestigioso percorso universitario. Grazie per avermi supportato in qualsiasi momento senza mai farmi mancare nulla e per avere sempre creduto in me. Spero di potervi restituire un giorno tutto quello che mi avete dato. Farò tesoro di tutto ciò che mi avete trasmesso e che ho imparato.

"Abbiate il coraggio di seguire il vostro cuore e la vostra intuizione.
In qualche modo loro sanno che cosa volete realmente diventare.
Tutto il resto è secondario."

Abstract

In recent times there has been considerable interest in the development and improvement of renewable energy. Wind energy is one of the most encouraging and exponentially growing sources and together with other renewable energies will be fundamental for future energy demand. For this reason, the nominal power and size of wind turbines increase continuously as well as their complexity, due to the fact that the higher flexibility of the structural components ignites a fully aero-elastic response of the system. The use of multidisciplinary optimization software has become a necessity to reduce loads, costs and to increase energy production.

The aim of this project is to analyze a 20MW two-bladed turbine to highlight the possible advantages and disadvantages with respect to a standard three-bladed turbine with the same power. The first part of the work concerns the modification of the Cp-Max multidisciplinary optimization software to allow the code to also manage two-bladed turbine models. This category of turbines needs a teeter hinge, connecting the rotor to the hub, to allow the oscillation of the rotor around its plane, thus reducing the loads transferred to the hub and the tower. To estimate correctly the turbine performances, it is necessary to identify the azimuth angle at which the static analyses are performed. However, the most important code modification concerns the computation of the clearance between the tower and the blade tip. It is essential to update the computation procedure of this constraint as the teeter hinge allows the rotor to oscillate around its axis and consequently the blade to approach the tower. The clearance is the sum of the deflection of the blade and the displacement due to the teeter angle. After these modifications, Cp-Max can also deal with two-bladed turbines and the optimization modules can be used to design the machine.

The second part of the work concerns a design step-by-step of a two-bladed 20MW upwind wind turbine. The advantage of having one less blade involves a reduction of the AEP, as a consequence it is necessary to modify the external shape of the blade changing the solidity of the rotor. This procedure allows to improve the rotor aerodynamics and the energy captured. An additional step needed for a two-bladed turbine is the sizing of the stiffness of the teeter hinge. This has to be done by looking at the most critical conditions to obtain a reasonable maximum angle deflection of the hinge. Then a parametric analysis is performed comparing different combinations of up-tilt and stiffness of the teeter, by an optimization with the structural submodule of Cp-Max for each one of these combinations.

Finally, a preliminary comparison is made between a two-bladed and a three-blade configuration, observing the energy captured, the mass, the cost of energy and the loads, so as to understand the possible advantages and disadvantages of the two different configurations.

Keywords: wind turbines, two-bladed, teeter hinge, optimization

Sommario

Negli ultimi tempi c'è stato un notevole interesse per lo sviluppo e il miglioramento delle energie rinnovabili. L'energia eolica è una delle fonti più incoraggianti e in crescita esponenziale, e insieme ad altre energie rinnovabili sarà fondamentale per la futura domanda energetica. Per questo motivo, la potenza nominale e le dimensioni degli aerogeneratori continuano a crescere così come la loro complessità, dovuta al fatto che la maggiore flessibilità dei componenti strutturali implica una risposta aeroelastica di tutto il sistema. L'utilizzo di software di ottimizzazione multidisciplinare è diventato una necessità per ridurre i carichi, i costi e per aumentare la produzione di energia.

Lo scopo di questo progetto è quello di analizzare un aerogeneratore a due pale da 20MW per evidenziare i possibili vantaggi e svantaggi rispetto ad un aerogeneratore standard a tre pale di pari potenza. La prima parte del lavoro riguarda la modifica del software di ottimizzazione multidisciplinare Cp-Max per consentire al codice di gestire anche modelli di turbina a due pale. Questa categoria di turbine necessita di una cerniera oscillante, che colleghi il rotore al mozzo, per consentire l'oscillazione del rotore attorno al suo piano, riducendo così i carichi trasferiti al mozzo e alla torre. Per stimare correttamente le prestazioni della turbina, è necessario identificare l'angolo azimutale al quale eseguire le analisi statiche. Tuttavia, la modifica del codice più importante riguarda il calcolo della distanza tra la torre e la punta della pala. È essenziale aggiornare la procedura di calcolo di questo vincolo poiché la cerniera oscillante consente al rotore di oscillare attorno al proprio asse e di conseguenza alla pala di avvicinarsi alla torre. Il gioco è la somma della flessione della pala e dello spostamento dovuto all'angolo di oscillazione. Dopo queste modifiche, Cp-Max può anche occuparsi di aerogeneratori bi-pala e i moduli di ottimizzazione possono essere utilizzati per progettare la macchina.

La seconda parte del lavoro riguarda la progettazione passo passo di una turbina eolica bi-pala da 20MW con configurazione controvento. Il vantaggio di avere una pala in meno comporta una riduzione dell'AEP, di conseguenza è necessario modificare la forma esterna della pala cambiando la solidità del rotore. Questa procedura permette di migliorare l'aerodinamica del rotore e l'energia catturata. Un ulteriore passaggio necessario per una turbina a due pale è il dimensionamento della rigidità della cerniera oscillante. Ciò deve essere fatto osservando le condizioni più critiche per ottenere una ragionevole flessione angolare massima della cerniera. Quindi viene eseguita un'analisi parametrica confrontando diverse combinazioni di up-tilt e rigidità della cerniera, mediante un'ottimizzazione con il sottomodulo strutturale di Cp-Max per ciascuna di queste combinazioni.

Infine, viene effettuato un confronto preliminare tra una configurazione a due pale e una a tre pale, osservando l'energia catturata, la massa, il costo dell'energia e dei carichi, in modo da comprendere i possibili vantaggi e svantaggi delle due diverse configurazioni.

Parole chiave: aerogeneratori, bipala, cerniera basculante, ottimizzazione

Contents

List of Figures

List of Tables

List of Symbols and Acronyms

AEP	—	Annual Energy Production
AOE	—	Annual Operating Expenses
BEM	—	Blade Element Momentum Theory
$Beta$	—	Pitch angle position
$Beta_{dot}$	—	Pitch angle velocity
BR	—	Blade root
CoE	—	Cost Of Energy
C_p	—	Power coefficient
DLC	—	Design Load Cases
d	—	Horizontal displacement of the rotor
d_{dot}	—	Velocity of the horizontal displacement of the rotor
ECD	—	Extreme Change Direction
EOG	—	Extreme Operating Gust
ETM	—	Extreme Turbulent Model
EWS	—	Extreme Wind Shear
FCR	—	Fixed Change Rate
$HAWT$	—	Horizontal axis wind turbine
HC	—	Hub center
ICC	—	Initial Capital Costs
KPI	—	Key points information
LQR	—	Linear Quadratic Regulator
LUT	—	Look Up Table
MDO	—	Multidisciplinary Design Optimization
$MIMO$	—	Multi Input Multi Output
NTM	—	Normal Turbulent Model
Ω	—	Rotor Speed
PID	—	Proportional Integrative Derivative
SQP	—	Sequential Quadratic Programming
TB	—	Tower base
TSR	—	Tip speed ratio
TT	—	Tower top
$VAWT$	—	Vertical axis wind turbine
v_i	—	Cut-in Velocity
v_o	—	Cut-out Velocity
v_r	—	Rated Velocity

Chapter 1

Introduction

1.1 Context and Motivation

In recent times there has been considerable interest in the development and improvement of renewable energy. The significant growth in global energy demand and the environmental issues of fossil fuels supplies, along with the development of systems increasingly promising and technological as for performance and energy costs have all led to focus on renewables. In particular, wind energy is one of the most encouraging and exponentially growing sources in terms of size and power of machinery, and together with other renewable energies will be fundamental for future energy demand.

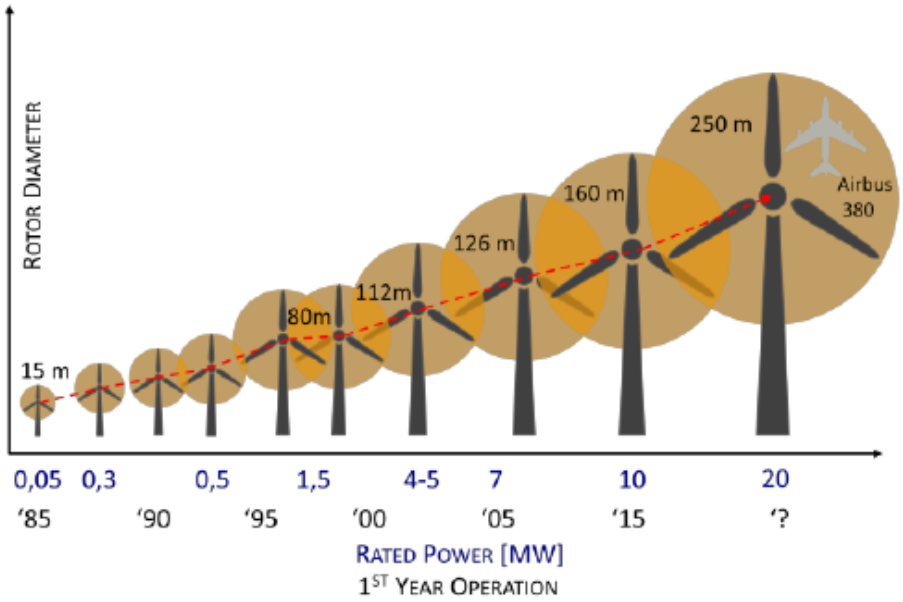

Figure 1.1: Up-scaling wind turbines [16].

The knowledge and the study of wind properties are essential for a full understanding of wind energy. The initial energy available and the actual ability to be exploited to the fullest will depend on wind features. Furthermore, the most evident characteristic of wind is its variability, in terms of place as well as time. This innate changeable nature of wind persists over a very wide range of scales, making the geographical choice essential for the installation of wind turbines. [11].

The interest in the construction of wind turbines has grown significantly in recent years and this has led to the development of methodologies and technologies for the design of a new generation of wind turbines. In particular, the optimization of the integrated aero-servo-elastic design proved to be the best approach among many other different methods. Therefore, multidisciplinary approaches have become fundamental, as they enable to model more and more features during the project itself. This leads to the realisation of lighter turbines, with technological and economic advantages compared to those of the previous generations. Interdisciplinarity between structure, aerodynamics, hydrodynamics and control brings advantages not only to the individual modules, which can interact with each other, but also to the overall design, being more complete and faithful to reality. This has led to the development of ever larger, more efficient and safer machines.

All types of wind turbines are made up of: a rotor that has the task of transforming the kinetic energy of the wind into mechanical energy, a generator that has the task of transforming mechanical energy into electrical energy, a support structure that has the task to keep the rotor in the correct design position, a control system that manages the operation of the machine and a connection to a central that deals with energy management [25].

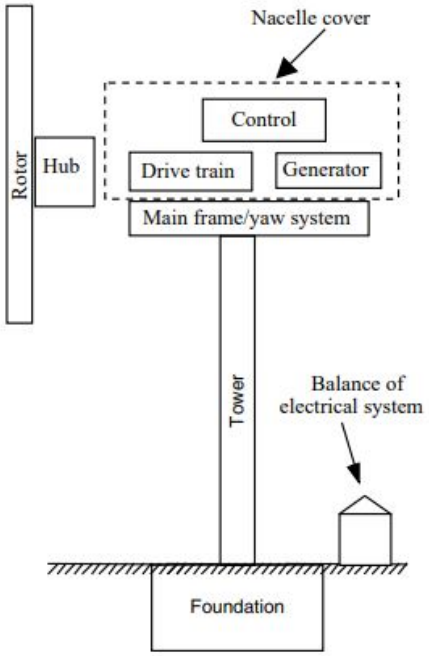

Figure 1.2: Wind turbine components [11].

There are different types of wind turbines that can be classified according to their features. The main differences concern the positioning of the rotor axis of rotation, which can be vertical or horizontal, and the positioning of the rotor with respect to the tower and the direction of the wind, which can be downwind or upwind [25]. The most common and most developed wind turbines in recent years are those with a horizontal axis of rotation (HAWT) upwind. They are preferred to vertical rotation axis machines (VAWT) in multi-megawatt applications for several reasons, the most important of which is the efficiency in capturing energy. They are also preferred to downwind configurations, which despite having the advantage of being dynamically stable and not having problems

of minimum distance between blade and tower, have the disadvantage of seeing the shadow of the tower and the consequent turbulence generating irregular loads on the blades.

Another important issue and key point of this work is the number of blades that make up the rotor. This directly affects the solidity of the rotor and consequently the performance, loads and cost of the wind turbine. The most common configuration is the three-blade upwind, because it is a good compromise between all the advantages and disadvantages of the number of blades. Three blades have the particular advantage that the polar moment of inertia with respect to yawing is constant, and it is independent of the azimuth position of the rotor. This characteristic contributes to relatively smooth operation even while yawing. However, a two-bladed rotor has a lower moment of inertia when the blades are vertical compared to when they are horizontal. This 'imbalance' is one of the reasons why most two-bladed wind turbines use a teetering rotor. Using more than three blades could also result in a rotor with a moment of inertia independent of position, but more than three blades are seldom used. This is primarily due to the higher costs that would be associated with the additional blades. In figure 1.3 it is shown the trend of the power coefficient with respect to the tip speed ratio with a different numbers of blades. A key consideration in selecting the number of blades is that the stress in the blade root increases with the number of blades for a turbine of a given solidity. Thus, all other things being equal, increasing the design tip speed ratio entails decreasing the number of blades. A few single-bladed turbines have been built in the last thirty years. The presumed advantage is that the turbine can run at a relatively high tip speed ratio and that the cost should be lower because only one blade is needed. On the other hand, a counterweight must be provided to balance the weight of the single blade [25].

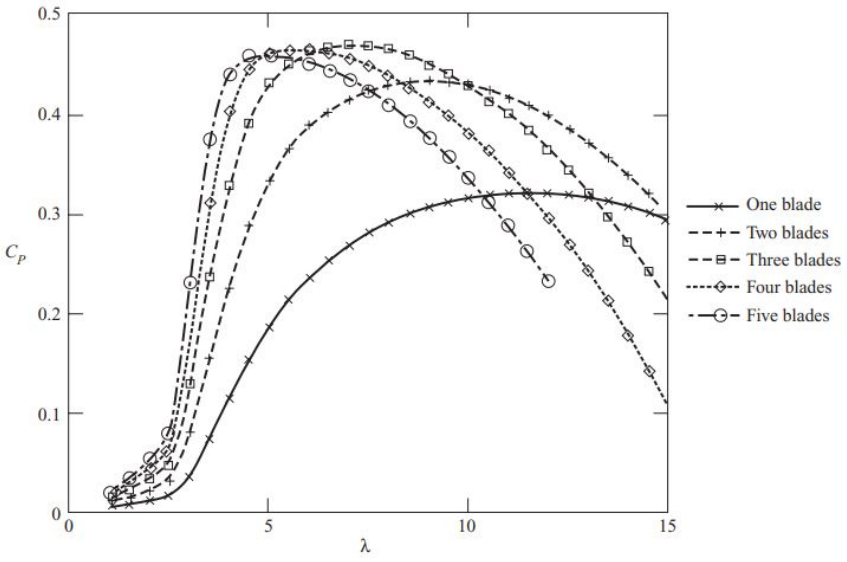

Figure 1.3: Effects of changing the number of blades on the power coefficient with respect to the TSR [11].

1.2 Objectives

The main purpose of this thesis is to develop the model and to do an analysis of a two-blade wind turbine with a nominal power of 20MW. However it is a configuration elaborated for research and not for a current design case, due to unprecedented characteristics.

The simulation program used for modeling and for verifying the operation of the turbine is Cp-Lambda [9], while the optimization software is Cp-Max [8] [32]. In order to interface with two-blade models in the Cp-Max software, some code parts were developed. This was necessary firstly to correct the model due to the different configuration of the turbine and secondly to adapt some operations of the different routines as a means to automate them. In particular, a configuration of mobile hub, typical for two-blade turbines, was modeled in the Cp-Lambda model. In addition, it has been upgraded to estimate more accurately the turbine's performance. Finally, the means for reaching the minimum admissible distance between the tip of the blade and the tower has been completely redefined. This final phase is fundamental for the correct verification of the constraint and for the final certification of the machine and has been the main part of this work.

The two-blade model was developed starting from a 20MW three-blade machine as a reference model, a case study of the Politecnico di Milano. The project starts by simply removing a blade from the reference model and adding a swing hinge with initial features taken from a previous work. The task then continues with an analysis on the solidity of the rotor to consider the removal of one of the blades from the previous model and a consequent modification of the external geometry of the blades. At this point, the aim is to create a solution that exploits the advantages without weighing too much on the stiffening of the blades, as a means to guarantee complete compliance with the constraints. For this purpose, the teeter hinge is dimensioned. Then, a parametric analysis is carried out to compare different configurations of up-tilt angle and stiffness of the torsional spring, using the structural optimization module. Finally, the initial three-blade model is compared with one of the best two-blade models obtained, evaluating the advantages and disadvantages of the various configurations, comparing the cost of the energy and making the relative conclusions and considerations.

1.3 State of the art

1.3.1 20MW wind turbines.

Modern wind turbines are characterized by large rotor sizes and by a power production in the range of several megawatts. The classical procedure when designing a larger rotor is to draw an attempt solution by up-scaling an existing one. With this aim, two different approaches are usually adopted: linear scaling laws or existing data. The approach that uses linear scaling laws is largely discussed in literature. Generally, it was found that upscaling using existing materials and design concepts will result in massive wind turbines that are economically inferior to the existing state of the art. Nowadays, the application of these methods fails to give an overall impression in the conceptual design phase, while technical feasibility and economical characteristics may not be accurate enough to make a realistic judgment about the design (due to the inherent assumptions and simplifications). However, a well-done up-scaling approach can give a good initial guess and helps the optimizer to search in a smaller design space, which consequently reduces the overall computational time. The main drawback of using an up-scaling technique is the unclear effect that it has on the overall behaviour of the turbine. It must be checked if the trade-off between the higher power production and the mass (and loads) increment is favourable or not. Here an integrated aeroservoelastic simulator comes into play as a useful tool to address this issue.

Much research has been carried out to investigate the ability of classic numerical models to deal with increased level of aero-structural complexity for 10-20 MW wind turbines, with its implications on the design of components. The activities of the INNWIND.EU project covered a variety of studies concerning the development of conceptual 20MW wind turbines [12] [6] [26] [29]. Concerning the design process, reference 20 MW solutions have been tentatively proposed in literature in the past years. In particular, Peeringa [27] proposed a preliminary description of a 20 MW wind turbine, including the aerodynamic and structural characterization of the rotor and fundamental integrity verification. In this work the classical up-scaled 20MW wind turbine, based upon the Upwind 5MW reference wind turbine, is used as a starting-point for the design. The blade and control design was done in two design iterations. In the first iteration the absolute (scaled) blade thickness is applied. In the second iteration the relative blade thickness is applied together with a Reynolds correction for all the airfoils. The aeroelastic model of the wind turbine is a mixture of up-scaled wind turbine data and the output of the rotor and control design [28]. In a recent work, Ashuri [4] employed multi-disciplinary optimization algorithms to perform a common aeroelastic definition of a 20 MW reference wind turbine, in which several global and specific features of the rotor and the tower are designed in order to minimize the LCOE.

In recent times, hard work has been committed to the development and validation of automated design algorithms. This usually integrates high-fidelity physical models with dedicated numerical optimization techniques with the aim to provide significant help during each phase of the design, from preliminary system characterization to the detailed sizing of specific components. These methods lead to conduct dedicate studies and trade-off analysis, which can help in identifying promising trends and solutions for technological innovations and for the reduction of capital and operating costs. [31]

1.3.2 Two-bladed wind turbines.

In recent years, the three-bladed wind turbines have been the most common, and despite this, different types of two-bladed wind turbines have been developed in the past. The first significant two-bladed turbine dates back to the 1930s and it was a 1.25MW turbine [30]. During the 1970s and 1980s, in response to the increase in oil prices, NASA started to develop several wind turbines. During the following years United Technologies Corporation and General Electric also developed two-bladed turbines until the early 1990s, when three-bladed wind turbines became the best choice in the years to come. In the 2000s different companies started developing and building two-bladed wind turbines mainly for off-shore applications.

The progress of these machines was also permitted by the technological development of the materials and of the control systems, including active and passive solutions. The aim of all companies has always been to develop turbines reducing the cost of energy. The Chinese manufacturer Envision developed wind turbines from 2 MW up to 6.5 MW. In 2008 it produced a 3.6 MW two-bladed wind turbine, with a rotor diameter of 128 m and an operative range between 3 and 25 m/s [38] [15]. In 2016 in The Netherlands, 2-B Energy developed and installed the 2B6, a 6 MW wind turbine with a nominal speed of 13 m/s [38]. The turbine was designed for both onshore and offshore applications. The preferred solution has been the offshore due to its noise, despite being more expensive. In 2017 another Dutch company, Seawind Technology, developed a 6.2 MW two-bladed wind turbine for offshore applications. Starting from this configuration, an up-scaled machine with a nominal power of 12.2 MW has later been developed. The diameters of these two machines are respectively 126m and 225m, and designed to be offshore floating solutions [36]. They will be commercially available starting from 2023 and 2024. Other examples of companies which have developed two-bladed turbines are the French Vergnet Eolien [37] and Windflow Technology from New Zeland. Both of these companies carried out onshore and offshore solutions with a nominal power up to 1 MW. A significant project of the French company is the GEV HP, a turbine with a delta-three teetering hub that allows to reduce the loads caused by turbulence.

There are some study cases of two bladed turbines available in literature as well. A master thesis from Delft university dated 2010 [3] compared three-bladed and two-bladed wind turbines with the goal of establishing which was the most cost-effective. The largest turbine analyzed was 10 MW and the overall results suggest that with the same tip speed ratio the three-bladed had a lower energy cost, whereas with no limits on the tip speed the two-bladed was more convenient. Another important conclusion was that the energy yield of the two-bladed was lower and the support structure cost was higher. Another reference has been found in the article written by Bossany and published in 2013 [7]. The focus of this work was to design a control system to reduce the structural loads for a turbine with a nominal power of 600kW. Specifically, the controller supervised an individual pitch system to compensate for asymmetrical loads caused by non-uniform flow across the rotor. This resulting load reduction demonstrates that it is possible to design larger, lighter, and more flexible two-bladed structures. In the thesis paper of Civati [13] from Polimi, a study was conducted on the design of a 10 MW two-bladed wind turbine, comparing it with three-bladed turbines to evaluate the best solution. The peculiarity of this work was the tower redesign, performed by adding a tuned mass damper to reduce oscillations and by introducing post-tensioning tendons to increase the stiffness.

The two-bladed wind turbines is certainly an appealing field to develop and expand for companies interested in renewable energy. Innovative technologies applied to recent projects can lead to a potential reduction of the cost of energy.

There are several studies of 20MW wind turbines and different cases of two bladed turbines as well. However, it is difficult to find study cases with both characteristics especially for working machines. For example, in the 2019 article [1] there is a comparison between a two-bladed and a three-bladed 20MW offshore turbine, displaying the advantages of the two-bladed configurations. Another reference is the preliminary design of a two-bladed turbine developed at PoliMi by Giulianini in her work of thesis [20] published last year.

Chapter 2

Cp-Max Code and Optimization

2.1 Architecture and Optimization Code

A multi-disciplinary design suite Cp-Max was used to design a wind turbine in this project. (Code for Performance Maximization)

The code is based on the combination of highly detailed numerical models with a multi-level architecture: a macro design loop manages the optimization of the submodules by changing the main characteristics of the turbine, which are sized with the goal of minimizing the CoE.

The optimization is built on several MATLAB routines and the core of the code is Cp-Lambda (Code for Performance, Loads, Aeroelasticity by Multi-Body Dynamic Analysis). Cp-Lambda is an aero servo elastic multibody-based code whose focus is to simulate the static and dynamic behaviour of the machine under numerous conditions. The code is multibody-based because it contains a library of elements (flexible beams, rigid bodies, sensors, actuators, joints, springs, dampers...) that can be combined according to the configuration and to the machine analyzed. In figure 2.1 it is shown how a three-bladed model is composed.

The code is based on the blade element momentum theory (BEM) and according to the annular stream-tube theory. With this model it is possible to take into account several aerodynamic phenomena, including wake swirl, tip and hub losses, unsteady corrections, and dynamic stall.

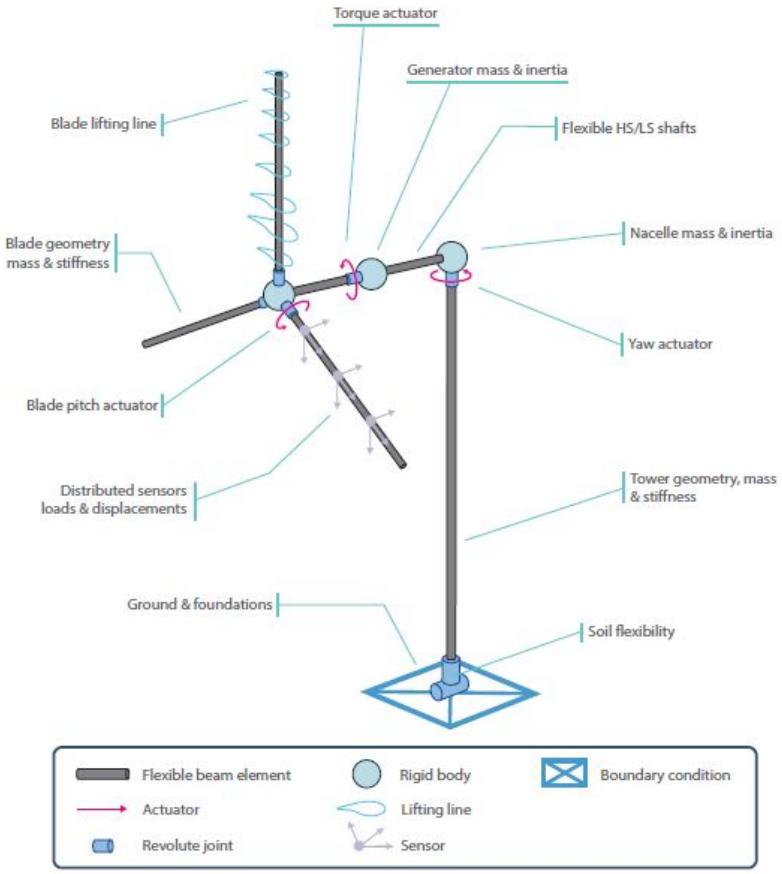

Figure 2.1: Topological description of a wind turbine [32].

The main design loop is the Macro Design, which is the outer loop of the optimization. The variables taken into account are called macro parameters because they are the ones that affect most the design and the performance of the machine. The macro parameters that can be included in the optimization are the rotor diameter, the hub height, the rotor solidity, the rotor tapering, the thickness area, the thickness weighted area, the tip speed, the cone angle, and the tilt angle. For each perturbation of a macro parameter, the other more specific parameters can be modified and included in the optimization of the different internal submodules. The main submodules are the following ones, and in figure 2.2 the design framework composed by all the submodules is shown.

- The Aerodynamic Design Sub-module optimizes the aerodynamic shape of the blade by maximizing the AEP.
- The Control Synthesis Tool sets the controller type, choses the strategy of control for the operating envelope and creates the control laws.
- The Prebend Design Sub-module estimates the out of plane bending of the blade in order to maximize the rotor area in operative conditions.
- The Structural Design Sub-module sizes the structural elements of blades and of the tower in order to minimize the ICC.
- Other more specific Sub-modules that can be included are the 3D FEM analysis and the Acoustic Analysis.

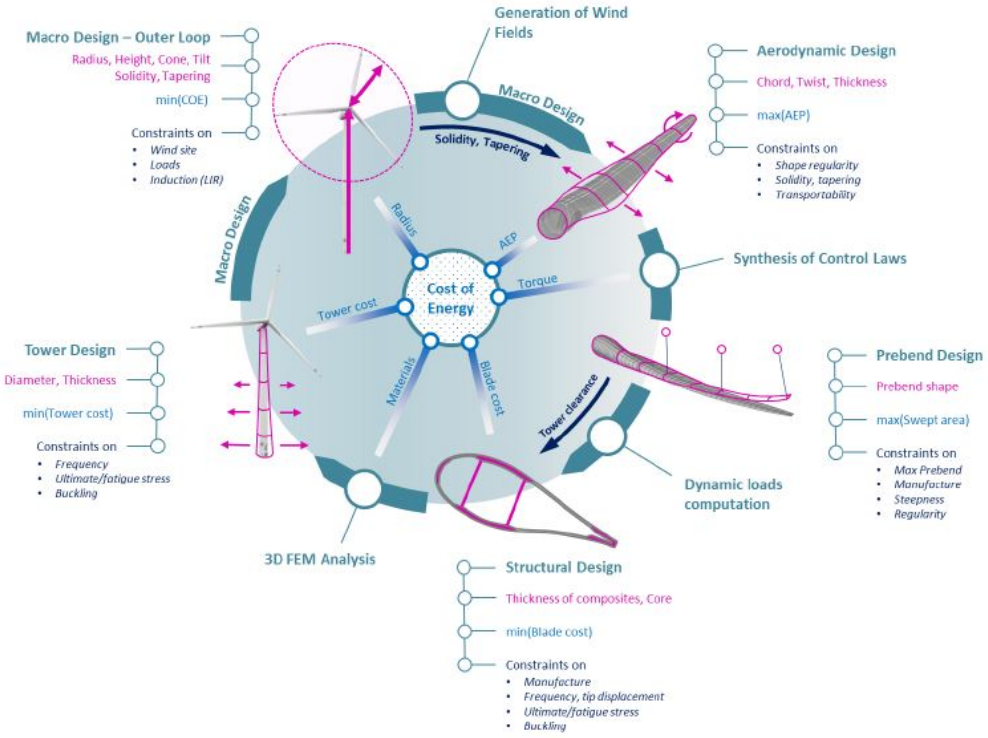

Figure 2.2: Design framework of Cp-Max [32].

A typical full optimization begins with the selection of the macro parameters to optimize. Consequently, by selecting one parameter at a time the inner loop begins. The data of the selected wind turbine are read by some MATLAB routines and an open-source code, TurbSim [24], generates the turbulent wind time histories for the specific machine, referring to the hub height, the rotor diameter and the wind class. The aerodynamic loop optimizes the external shape of the blade to maximize the AEP and then the control synthesis tool analyses the performance of the turbine and creates the control laws. The prebend module gives the best out-of-plane distribution to the blade to maximize the working conditions efficiency and then all the Design Load Cases selected are computed by Cp-Lambda. The structural design submodule reads the data of the DLC captured by the sensors and optimizes the blade structural elements according to the constraints, to minimize the ICC. If a more detailed structural analysis is required, a 3D FEM analysis is used as verification. When the optimization of the blade is finished, a structural optimization is made also on the tower considering all the modifications applied to satisfy the constraints and to reduce the ICC. Finally, when all the sub-modules find their optimum parameters values and the constraints are all satisfied, the micro-loop is considered finished and the CoE is calculated. The optimization process continues changing one of the active Macro Design variables and the overall optimization stops when the code finds a minimum for the CoE. For more details on the Cp-Max optimization architecture, in the Ph.D. thesis of Sartori [32] a design process is explained in detail. In the following subsections, the submodules of the code are briefly explained.

2.1.1 Aerodynamic Submodule

This tool is usually the first run because it modifies the external shape of the blade intending to maximize the production of energy, so the AEP. This submodule is based on the optimization of the chord, the twist, and the thickness of the blade, without changing the internal structure and thickness of the components. In this way, all the DLC are not computed and this allows us to save a lot of computational time. This is possible only if the blade is changed slightly, otherwise, it's necessary to redesign the internal structure of the blades. The aerodynamic loop is summarized in figure 2.3.

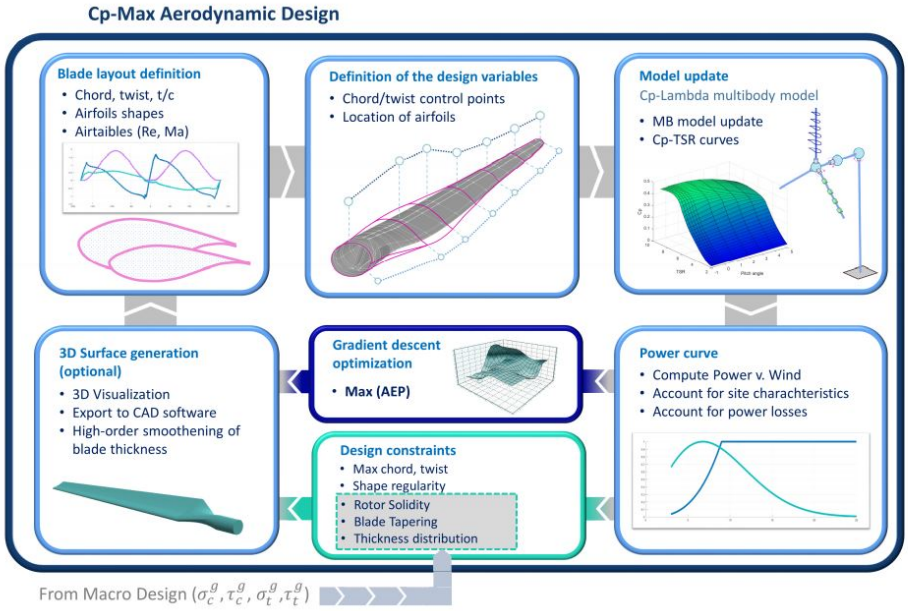

Figure 2.3: Design framework of the aerodynamic loop [32].

During this process the macro parameters are imposed, and taking into account these constraints, the optimization searches the best shape configuration to maximizes the AEP, by using the gradient-descent SQP method. This is done assuming that the merit function is sufficiently smooth for the various design variables. Bumped functions are used for the cord and the twist, so after the definition of the parametrization of the profile, the algorithm changes directly the bump between each interval. On the contrary, the optimization of the thickness is made by moving the profiles and then re-interpolating all. At every modification of the model, a set of the Cp-TSR is computed at the reference speed of to the turbine class. This gives an aero-structural performance surface that allows to figure out accurate control laws and a significant estimation of the AEP.

2.1.2 Control Synthesis Tool

This tool aims to create the control laws that govern the wind turbine during all the possible conditions encountered during its operational life, including nominal operating conditions, the occurrence of faults, gusts and parking conditions (refers to figure 2.4).

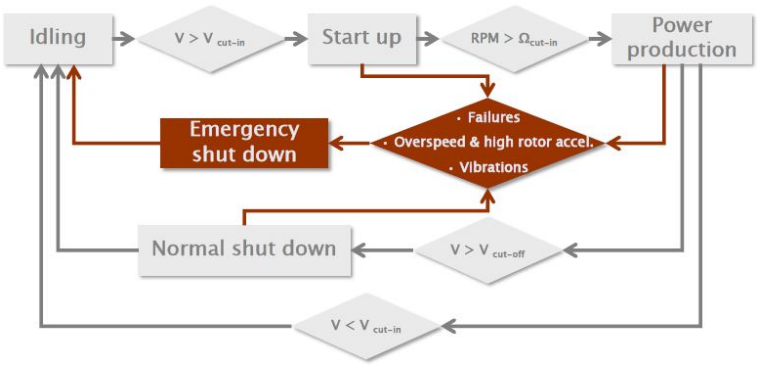

Figure 2.4: Operational states [14].

After the aerodynamic optimization, this submodule computes the static performance of the machine by using CpLambda to compute the Cp-TSR curves, and once they are computed the regulation trajectory is computed. Different strategies can be used for the determination of the regulation trajectory, but the majority of the wind turbines used in Cp-Max are pitch/torque controlled.

The main strategies and controller that can be used are:

- PID on collective blade pitch + LUT on torque
- PID on collective blade pitch + PID on torque
- Model-based control of pitch, torque

The PID controller is the most robust one because it works in the highest efficiency conditions only by knowing the rotor speed as input and then by adjusting the torque, according to the three characteristic gains. However, it is not always possible to use only a PID controller based on the rotor velocity, as a new region strategy is needed due to the maximum tip speed velocity. In this case, it is used a LUT to deal with this region, between the maximum Cp region and the power rated region.

Another more sophisticated controller is the model-based one. A reduced model is created and more states are used to control the machine. A MIMO LQR controller with 6 states and 2 inputs is used, but it is also possible to include the integration of the rotor speed as an additional state. This type of controller is typically used for big turbines where it is necessary to control more parameters.

2.1.3 Prebend Design Submodule

This tool has been implemented in one of the last versions and can be considered a part of structural optimization. The idea is to optimize the native out of plane deformation of the rotor to maximize the energy production during nominal operative conditions when the blades are deformed. [33] In mathematical terms, it is necessary to minimize the area between the rotor plane and the deformed blade. An idea of the entire process is shown in figure 2.5.

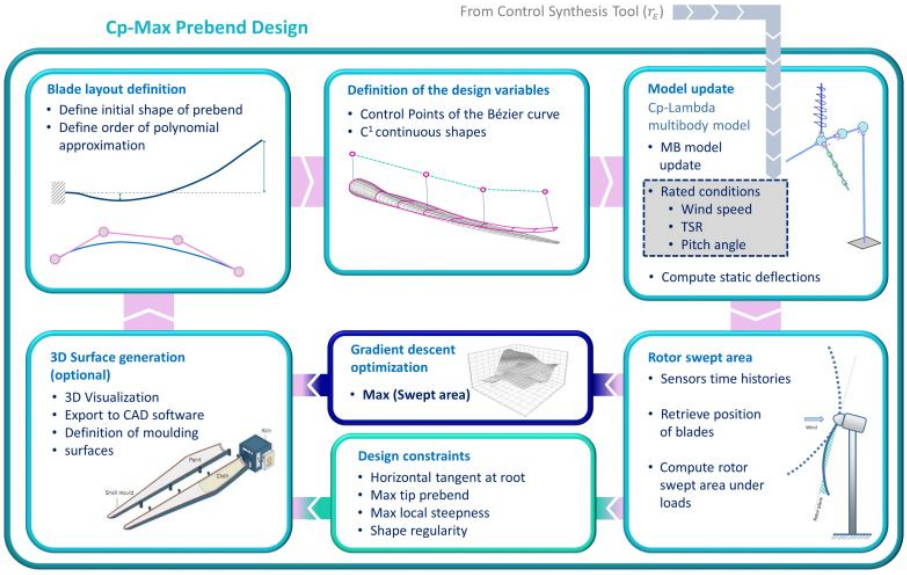

Figure 2.5: Prebend design architecture [32].

It is fundamental to define the upper and lower limits for the prebend as constraints and then define the control points along the chord for the optimization that uses the Bezier curves. This method is flexible, robust, and arbitrarily complex. However, it has the disadvantage of not being able to describe a prescribed geometry, so if a curve is given it is necessary to make an approximation that does not give the same result.

Generally, the constraints related to the limits on the displacements are related to the manufacturing process that usually has to be used for more than one turbine, so it can present limits due to the complexity and the costs. However, the use of the prebend enables a lighter structure, thus a good balance between complexity, optimization, accuracy, and costs must be attained.

The optimization process does not require DLC but only static simulations. This is usually carried out with 6 control points only for one blade, as the results should be very similar for all blades. This is completed in a short computational time.

2.1.4 Structural Design Submodule

The structural loop is considered the core of the optimization [10]. It is divided into two parts that can be run separately, the sizing of the blade structure and the sizing of the tower structure. It is the most complex and time-consuming section because it is necessary to compute the dynamic load cases to identify the most critical operative conditions and to size the internal structure respecting the constraints, intending to minimize the costs of the rotor and the tower.

The beams that compose the model have nonlinear properties and are described by FE with a 6x6 matrix for the mass and stiffness properties. The resulting model is very accurate if compared for example with the one that employs the software Fast using only 4 or 5 modes to describe the dynamics. The disadvantage of this accuracy is the CPU time needed for all processes.

The idea of this module is to design completely the internal structure of the blade. Therefore, after the definition of the components, the sizing is made by changing the distribution of thickness of each component, respecting the fixed external geometry. The variables that change during this loop are in the order of 100 and each one has upper and lower limits imposed by the user.

The submodule changes the structure and checks the loads, the fatigue, and the displacements trying to find an optimal solution that minimizes the ICC, which is a function of the blade mass. This procedure has to deal with the main design constraints:

- Resonance. It is necessary to check the first flap wise and edge wise frequency and the operative frequency, which depend on the number of blades, to avoid resonance problems.

$$f_{1st}^{flap} \geqslant n_B P$$

$$f_{1st}^{edge} \geqslant f_{1st}^{flap}$$

- Displacement. It is necessary to avoid the contact between the tip of the blade with the tower.

$$\delta_{blade} \leqslant \Delta_{blade/tower}$$

- Stress and strain ultimate. For every direction it is necessary to have lower stress and strain values with respect to the maximum admissible.

$$\sigma_{max} \leqslant \sigma_{adm}$$

- Stress and strain for fatigue. Check the fatigue loads from the normal operative conditions and respect them in relation to an index.

$$\sigma_f \leqslant 1$$

- Buckling. Check the instability shape on the beam in case of a compression load.

$$b \geqslant 1$$

All the constraints have to be satisfied and all have a safety constraint imposed by the guideline for the certifications of wind turbines [21]. The architecture of the code is summarized in figure 2.6.

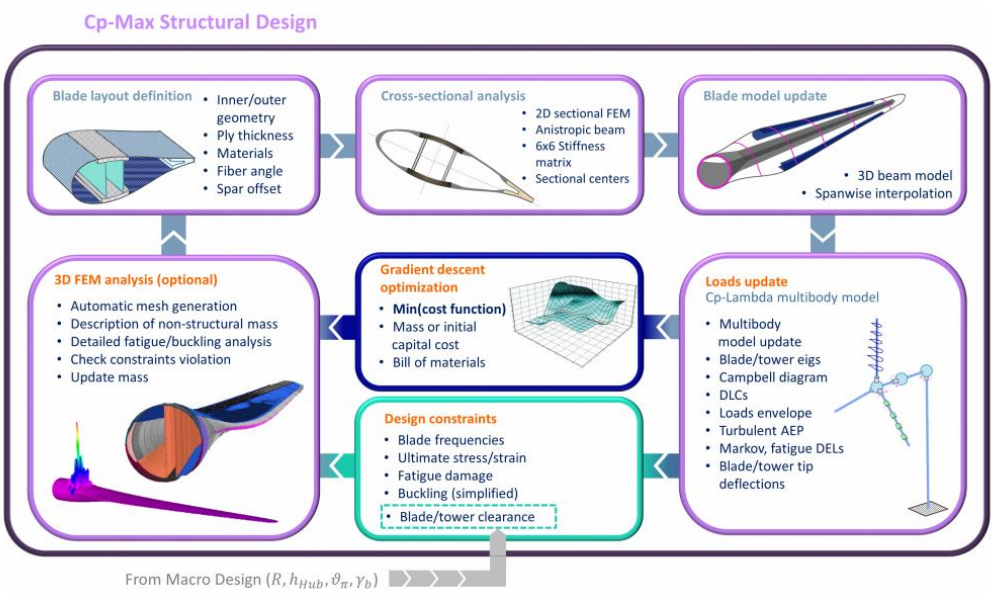

Figure 2.6: Structural design architecture [32].

The procedure starts from the definition of the model, previously computed, and the first passage is the computation of the turbulent and stochastic winds, using TurbSim [24] and some MATLAB routines. After this, CpLambda is ready to run all the selected design load cases and save as output the displacements, the loads and the fatigue DEL. Then the loads for the tip displacements are computed and a full fatigue analysis is run. Now the optimization process begins by using the MATLAB fmincon routine. At the end of the structure modification, a full fatigue analysis is run and the mass of the blade and the ICC are computed.

The most time-consuming operations are the fatigue analysis and the computation of the displacements. To deal with these problems after the computation of the DLC, the condition of maximum displacement is identified and the loads applied to the structure are reconstructed. In this way, at each structure variation, this reconstructed load is used instead of recomputing all the DLC. A similar approach is used for the fatigue analysis. The fatigue is evaluated in all the points during the full fatigue analysis, which is run at the beginning of the optimization. A table of priority is computed selecting the points with the high fatigue loads, and at each iteration optimization, a partial fatigue analysis is computed only on these critical points.

During all these processes the blade model used is composed of panels, and each panel has a structural description. Each variable is defined along the blade to describe its distribution. The higher the number of points that describe the blade, the better is the description of the structure but the higher is the computational time. So it is necessary to identify a compromise between precision and CPU time.

A more specific description of the blade is shown in figure 2.8 and in figure 2.7.

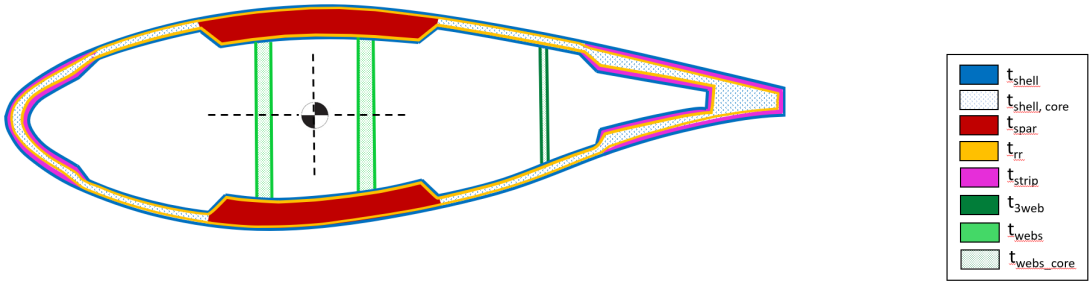

Figure 2.7: Materials description of the blade [32].

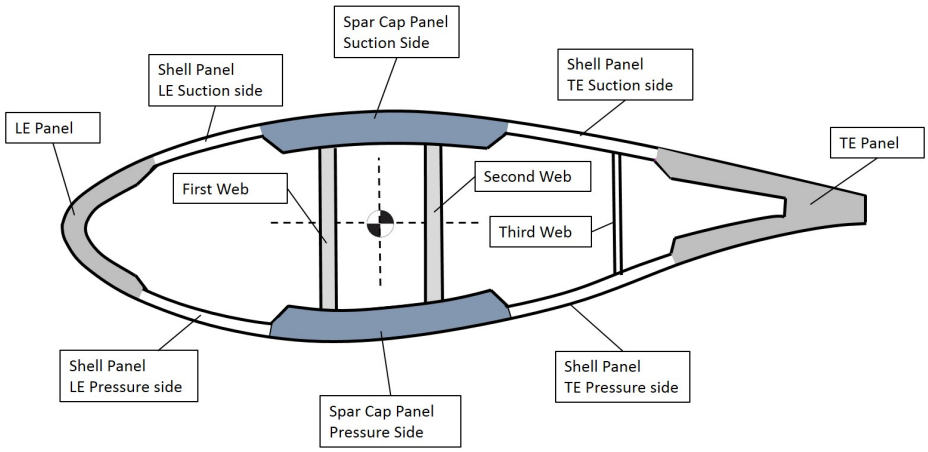

Figure 2.8: Structural description of the blade [32].

The main components of the blade are the shell panels (4), the spar caps (2), the shear webs (2/3) and the reinforcements (3).

- The shell panels ensure the continuity of the section and determine the geometry of the blade. Their task is to re-distribute the load to avoid sectional deformations and to contribute to the torsional rigidity. Shell panels are usually sandwich layers in which a core is coated with two layers of triaxial material ($0\,\text{deg}$, $+-45\,\text{deg}$).
- The spar caps provide the main contribution to the section flapwise stiffness. Their task is to absorb the flapwise bending. The first flapwise frequency and the out-of-plane displacement largely depend on these components. They are usually laminated with unidirectional material with the fibers aligned to the direction of maximum stress ($0\,\text{deg}$).
- The shear webs provide the main contribution to shearing stiffness normal to the chord. Their task is to absorb the shearing forces and they contribute to torsional rigidity as well. Shear webs are usually sandwich layers in which a core is coated with two layers of biaxial material ($+-45\,\text{deg}$). Usually, the shear webs are two, but if the section has relevant dimensions and a piece of the blade requires more shear resistance, a third shear web can be added.
- The leading edge and the trailing edge reinforcements provide the main contribution to the edgewise stiffness. Their task is to absorb the edgewise bending. The first edgewise frequency and the in-plane displacement largely depend on these components. These reinforcements are usually made of unidirectional material.

As some components might be identical, Cp-Max allows to define identical elements. This way, only one of the twin components is optimized while the other is copied, slightly simplifying the optimization procedure and the time-consuming.

2.2 Cost Model

In the last section, all the submodules of the multi-level optimization process have been presented. Each one contributes to the overall optimization, but the main goal of Cp-Max is to optimize the design of a wind turbine minimizing the cost of the energy, the CoE, which is the most important parameter of the overall optimization.

The definition of CoE is in the following equation:

$$CoE = \frac{FCR \cdot ICC}{AEP_{Net}} + AOE \qquad \left[\frac{\$}{kWh}\right] \tag{2.1}$$

The FCR represents a fraction of the initial cost needed to cover the capital cost, return on equity or debt, and other financial costs; the ICC represents the sum of the turbine cost and the balance of station; the AOE includes the land lease cost, O&M, and replacement/overhaul costs; the AEP is computed concerning the turbine class and site-specific wind conditions.

This is the general definition for the cost of energy, but there are different models to compute the single costs. Two example of costs models are the "NREL Cost model" [18] and the "INNWIND Cost model" [22].

The main parameters of the cost model can be calculated from the knowledge of a few parameters of the wind turbine. The cost of each sub-component of the turbine is calculated based on the length and mass of the blade, the energy produced, and other parameters. The final costs are obtained through dedicated scale laws. Similarly, the costs for commissioning, operating, and decommissioning the plant can be calculated. The main limitation of this model is related to the reliability of the scaling relationships, which have been derived by fitting existing data from different projects in the past. Problems could arise using these models and existing scaling laws for estimating the cost of next-generation multi-megawatt turbines.

These empirical models can therefore be considered reliable if used for machines similar to the case study considered. According to this, the design of this 20MW turbine cannot be based solely on minimizing the cost of energy, as there are not many case studies similar to the analyzed case. Therefore, the cost model for a preliminary design phase can be considered a relative reference among the various configurations adopted but cannot be considered as an absolute parameter that can therefore be compared with cases that differ from this.

Another important aspect to consider is that no cost model was found for the teeter hinge implemented in the two-blade model analyzed. Therefore this aspect must be taken into consideration when comparing the two-blade configuration and the three-blade configuration, as it is certainly not a negligible cost being a relevant component of the hub.

2.3 Certification

This work is focused on a preliminary design of the turbine, so a selected set of DLC is used in the optimization design process to reduce the computational time. The choice of the DLC is done by taking into consideration all the possible operating conditions that a wind turbine encounters throughout its lifetime. As a further simplification, turbulent DLC was performed with only one seed, although in real-world applications several seeds are required for a comprehensive analysis.

The DLC used are summarized in table 2.1 according to their definitions as specified by the International Electrotechnical Commission, 2006 [23].

DLC	Wind	Other descriptions
1.1	NTM	
1.3	ETM	
1.4	ECD	
1.5	EWS	
2.1	NTM	+ grid loss
2.2a	NTM	+ grid loss + individual pitch freeze
2.2f	NTM	+ individual pitch runaway towards minimum pitch
2.3	EOG	+ grid loss
6.1	EWM50	
6.2	EWM50	+ grid loss
6.3	EWM1	

Table 2.1: List of DLC.

All the considered cases contribute to the definition of the ultimate loads, while only the DLC 1.1 is taken as a driver for the fatigue equivalent loads, as they are representative of the normal working condition of the machine.

The turbulent wind time histories are generated with the open-source code TurbSim [24], while deterministic gusts are generated by Matlab routines according to international standards. Some sub-cases of the DLC in table 2.1 have been excluded because of the difficulties in reaching the convergence. The simulations have been performed at the reference velocities, for the power production between v_i and v_o, for the deterministic cases at v_r and at v_o.

Chapter 3

Two Bladed Turbine

The core of this work concerns the analysis of a two-bladed wind turbine and its implementation during the optimization process in the Cp-Max code. The main difference between a two-bladed and a three-bladed turbine model is the architecture of the hub. In a two-bladed wind turbine, the hub is not rigid because a teeter hinge is added connecting the rotor to the nacelle, thus admitting a relative rotation between the two elements.

The introduction of this element is necessary because of the asymmetry of the rotor and the action of the wind shear. These causes extra bending moment on the hub with the same frequency of the rotation. Together with the loads deriving from yaw manoeuvres with horizontal blades (refers to figure 3.1), the result is a huge increment in the fatigue loads of the turbine. The most critical parts affected by this increase of the loads are the blade root, the hub, and the tower. This new component is added to reduce these load problems.

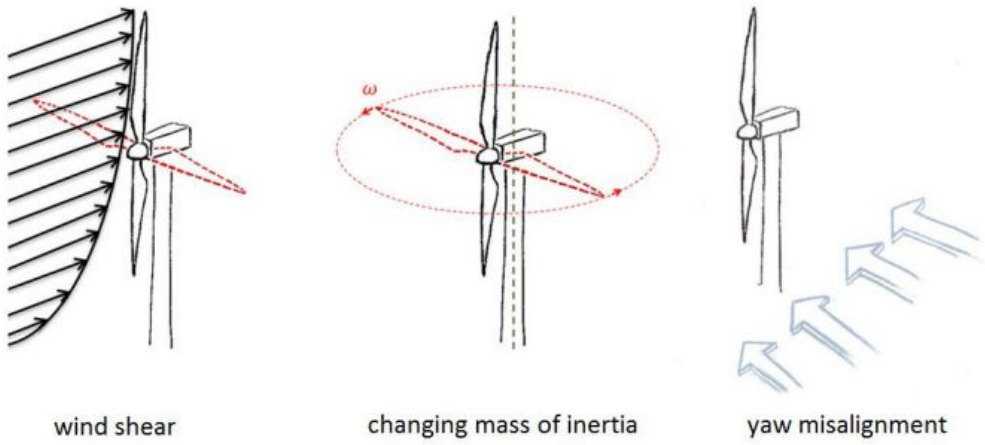

Figure 3.1: Sources of turbine loads [35].

Another problem related to the two-bladed configuration is the computation of the static simulation used to determine the performances of the turbine. According to the two-blade orientation, the azimuth position of the rotor affects the results. Therefore, it is necessary to find the correct azimuth angle that leads to compute the static analysis properly.

After including the teeter hinge, it is necessary to modify the Cp-Max code section where the maximum blade tip-deflection is evaluated to compute the clearance constraint, also including the displacement related to the deflection angle of the hinge. After including all these modifications in the code, the Cp-Max optimization can deal with a two bladed wind turbine and can be sued for a design process.

In this work, the machine used as initial guess in order to obtain a two-bladed configuration is a 20MW three-bladed turbine. After removing one blade it is necessary to modify the geometry of the two blades that constitute the rotor because the machine is significantly changed. The first aspect to be discussed is the modification of the solidity that affects significantly the performance and the response of the machine. For this reason, an analysis on the solidity variation is conducted. Another significant aspect is how the clearance between the blade tip and the tower change in function of the stiffness of the teeter which corresponds to different angles of maximum deflection. Thus, a parametric analysis is conducted, using as variables the up-tilt angle and the stiffness of the teeter hinge, with the goal of understanding how clearance changes and how the ultimate loads and fatigue DEL change.

3.1 Teeter Hinge

Following the conclusion that a teeter hinge connecting the rotor to the nacelle needs to be added to a two-bladed turbine, it is necessary to investigate how the teeter hinge is made and how it works. In figure 3.2 it is possible to see the main components of a teetering hub, while in figure 3.3 it is possible to view a particular example of teetering hub with a $\delta 3$ axis.

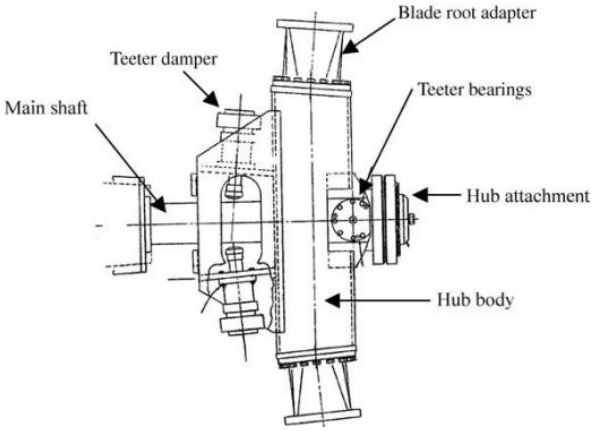

Figure 3.2: Components of a teetering hub [25].

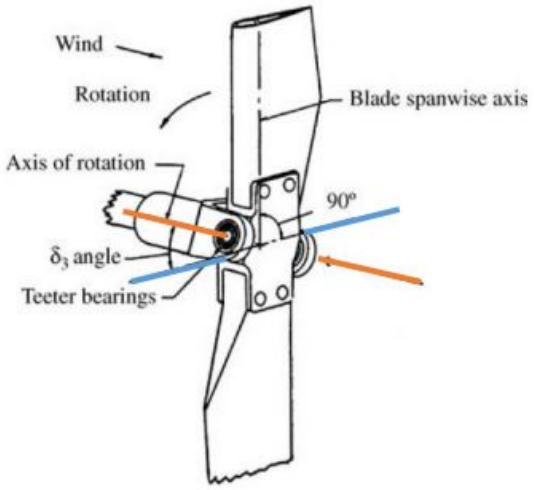

Figure 3.3: Teetering hub with a δ_3 axis [25].

The teetering hub is composed of a hinge with a torsional spring and damper that allows the rotor to rotate in the fore-aft direction reducing the out-of-plane bending moment fluctuations. The motion of the teeter is limited between a specific range of angles, in order to avoid extreme undulations on the rotor and to control the clearance between the tip of the blade and tower. It is possible to choose how the rotor can move and fluctuate around this hinge by selecting specific springs and dumpers. The properties of the spring and of the damper influence directly the behaviour of the oscillations. For example, the easiest configuration is a linear and symmetrical response of the spring

according to angle variation. From this condition, it is possible to change the response of some specific intervals by modifying the value of the linear stiffness, as well as to change the linear response of the spring into a quadratic response or to add an initial zero stiffness region. The spring can be selected in function of the requirements of the project, taking into account the complexity and the cost of its manufacturing process.

In this work of preliminary design, the spring is modelled with a linear stiffness constant in all the desired operating range. As a way to model the end impact, the stiffness is increased by some order of magnitude in a small angle range. The details of the implemented spring are shown in figure 3.4.

The sizing of the spring stiffness is necessary for every turbine configuration, depending on the geometry and on the mass of the model. In this work, the order of magnitude was acquired from the previous work done by Giulianini [20] selecting this configuration as initial guess. Then, in chapter 4, a manual and iterative sizing is performed, trying to reach a compromise between the advantages of a flexible hub and the disadvantages that reduce the clearance between the tower and the tip of the blade.

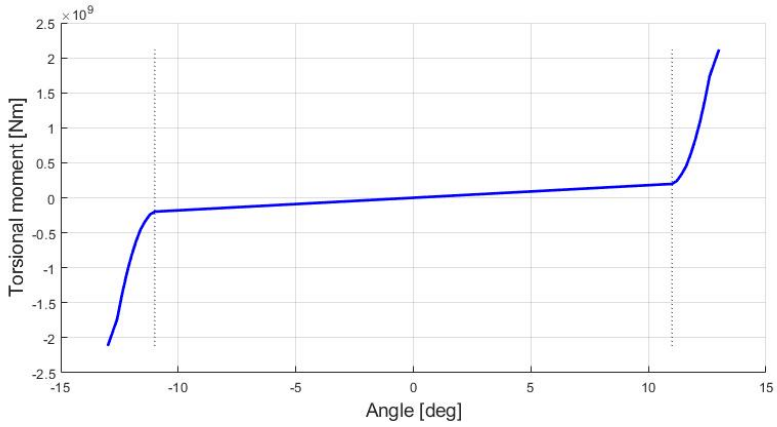

Figure 3.4: Teeter spring with linear constant $= 1.8 * 10^7 Nm/deg$.

As a means to add this new element in the optimization code, an if-else condition has been implemented: the code choses what model to use in the Cp-Lambda language, depending on the number of blades. Taking advantage of the multibody code architecture, a revolution joint has been placed between the hub centre and the drive train shaft. To easily modify the properties of the spring and of the damper, these data have been included in the Excel input file where it is possible to choose arbitrarily the number of points to describe the behaviour of the model.

3.2 Static Analysis Cp-TSR

As already stated, an important point to take into account is that a rotor composed only of two blades is not as balanced as a three-bladed rotor. The relative position of the rotor with respect to the nacelle and the tower, at which the static analysis are computed, affects the performance of the machine. This is related to the wind shear and to the effect of the tower shadow, which result in the generation of different loads depending on the azimuth angle. The final effect are different power coefficients and performance estimations.

In order to estimate properly the performance of the rotor and to compute the regulation trajectory, the Cp-TSR curves of the machine must be known. These curves describe at each configuration of TSR and pitch how much energy is converted from the wind into mechanical energy by the rotor. In this way it is possible to find the best configuration of pitch and rotor speed for every wind speed. To estimate these curves, it is necessary to compute some static parametric simulations with Cp-Lambda. As already said, because of the wind shear and the tower shadow, it is necessary to find the azimuth position, which estimates the real performance of the machine in the best possible way.

Starting from the work of Giulianini [20] a similar analysis has been made. Some azimuth angles have been selected from $0deg$ to $180deg$, with a step of $15deg$, to run the static simulations at these values. It has been decided to extend the original gap from $[0deg90deg]$ to $[0deg180deg]$ to better estimate the solution, because the response of the machine can be considered symmetrical in this type of analysis only with an interval of $180deg$ due to the geometry of the turbine. It has been selected a reference wind velocity close to the reference value of the site condition ($11m/s$), and a pitch angle close to the one that gives a maximum Cp ($\beta = -2deg$). In this way the computational time has been reduced with comparison to the run of the overall Cp-TSR-pitch curves.

Although the analysis is similar to the one made in the previous work [20], the final results are different. The azimuth angle that better approximates the mean value given from all configurations is $30deg$. The results are shown in figure 3.5. From the previous analysis the resulting azimuth angle that better approximates the mean Cp value was $90deg$. The differences could be related to different simulation settings or to an error in the data processing.

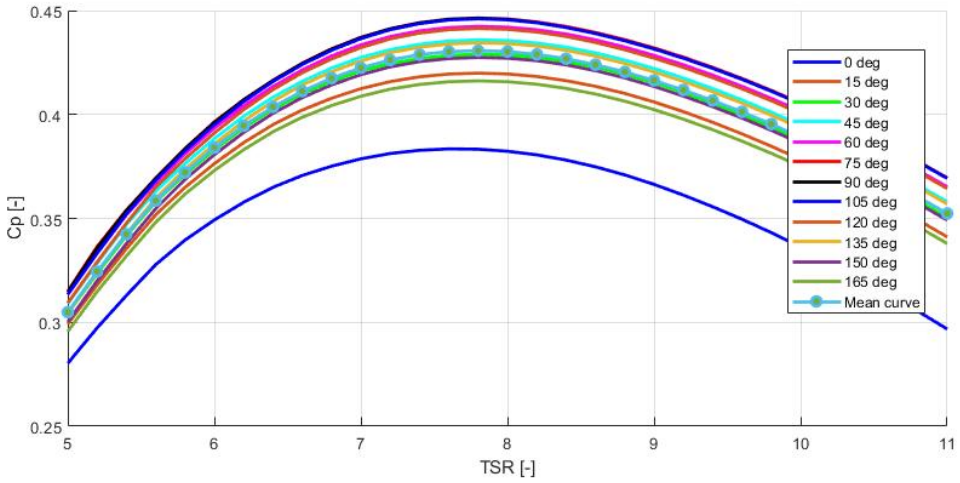

Figure 3.5: Cp-TSR curves ($\beta = -2deg$).

It was decided to find a better approximation of the azimuth angle that gives a curve as much as close to the mean one. So a refinement analysis has been done around the values that better approximate the mean value. In figure 3.6 it is possible to see that the curve at $35deg$ of azimuth is a reasonable estimation of the mean curve.

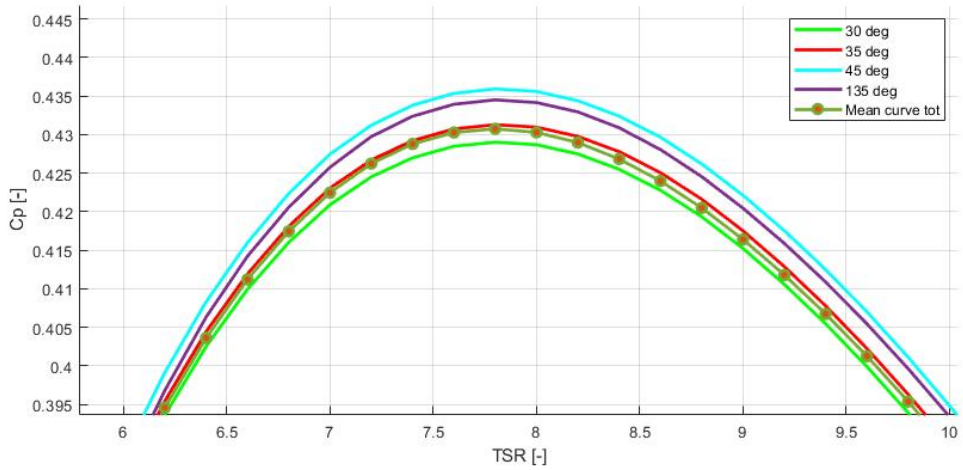

Figure 3.6: Cp-TSR and mean approximation curves ($\beta = -2deg$) .

In this way, it is supposed that the performances are well estimated, neither underestimated like for an azimuth angle of $0deg$, nor overestimated like for an azimuth angle of $90deg$. The automation and implementation of this feature in Cp-Max was thus considered appropriate: once the number of blades has been identified from the input file, the static simulations are carried out at the predetermined azimuth angle.

3.3 Tip Displacement

3.3.1 Definition of the constraint

The most important aspect to consider when dealing with a two-bladed turbine is that, with the introduction of a teeter hinge, the rotor plane can oscillate around the hub centre. The effect is that the rotor plane approaches the tower reducing the clearance between the tip of the blade and the tower. One of the main and important constraints that affect considerably the design of a wind turbine is the minimum clearance reachable between the tip of the blade and the tower. As mentioned in the guidelines for the certification of wind turbines [21] the minimum distance allowed is equal to 30% of the undeformed position. The main parameters that affect the clearance are the tilt angle of the nacelle, the stiffness of the blade, the overhang of the rotor, the cone angle, the prebend, and the maximum rotation of the teeter hinge.

To better understand this constraint, these are the definitions of the main geometry parameters of a turbine (reference to figure 3.7):

- The angle between the horizontal axis and the rotor shaft is defined as tilt angle; a positive angle increases the hub height and the tower clearance.
- The stiffness of the blade depends on its internal architecture, on the distribution of thickness of each component, on its external geometry and on the materials that compose it.
- The rotor overhang is the distance between the centre of the hub reference system and the intersection of the rotor axis with the tower centre line; for an upwind turbine, the rotor overhang is positive.
- The angle between the rotor plane and the blade axis is the cone angle.
- The prebend distribution describes the out of plane deflection of the blade; a positive prebend allows to move the blade away from the tower and optimizes the energy captured in the operative conditions.
- The maximum rotation of the teeter angle depends on the stiffness of the torsional spring and on the magnitude of the loads that act on the rotor.

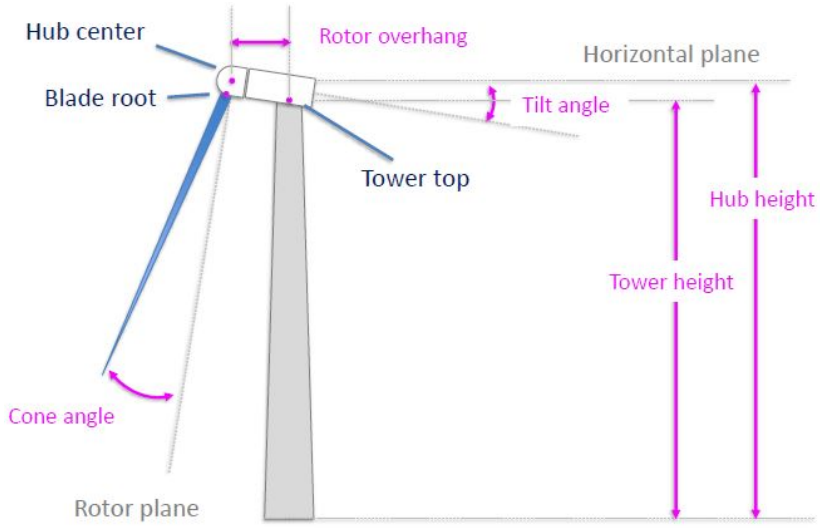

Figure 3.7: Turbine geometry [14] .

The Cp-Max code checks the computation of this constraint during the structural optimization of the blade: at each iteration the thicknesses of the internal components change so as to search a solution that satisfies all the constraints and minimizes the cost. Consequently, by changing the internal structure, the stiffness and all the properties of the blade change, so the constraints have to be recomputed every time.

The computation of the clearance between the tip-blade and the tower follows the next steps. After the computation of the dynamics simulations, the code identifies the load condition and the time step that maximizes the deflection of both blades. This corresponds to the closest position between the blade tip and the tower (usually searched at an azimuth angle between 150deg and 210deg). Once the load condition is identified, the code reconstructs a set of loads that are applied on a simplified model, composed of a blade hinged to the ground, which gives the same deformation to the blade as on the original model. During the structural optimization, as a means to reduce the computational time, the deflection is computed on the simplified model, on which the reference loads act at every structural modification. Then the clearance is computed at every iteration and it is compared with the maximum deflection that can be reached.

With the introduction of the teeter hinge in a two-bladed turbine, the computation of this constraint has to be changed. The main reason is that it is no longer possible to identify the minimum clearance reachable by the blade computing only the tip deflection, due to the fact that it is not the only parameter affecting the clearance variation. Therefore, it is necessary to compare the absolute positions of each tip blade at each time step to identify the condition of minimum clearance. After that, in a similar way, the loads of the extreme conditions have to be reconstructed and used as reference loads for the optimization. Consequently, it is necessary to modify the computation of the constraint during the structural sizing of the blade also taking into account the rotation due to the teeter angle.

3.3.2 New procedure and implementation

The implementation and the details of the procedure are explained in the following lines.

First of all, it is necessary to define some geometry parameters. Starting from the characteristics of the machine, it is necessary to identify a point on the tower to use as a reference for the definition of clearance between the tip of the blade and the tower. The height of the point is defined in the following way:

$$HTower = HubHeight - \frac{RotorDiameter}{2} \tag{3.1}$$

As the tower is defined by sections, in order to compute the radius of the tower at the selected height, it is necessary to interpolate between the sections of the tower. The coordinates of the reference point on the tower in the inertial reference are:

$$PointTower_{ine} = (HTower; -RTower; 0) \tag{3.2}$$

By using the definition of rotor overhang, up-tilt angle, pre-cone angle, prebend and blade length, the position of the tip of the second blade (the one with azimuth equal to 180deg) is defined. Then, the reference clearance of the undeformed structure is computed in this way:

$$ClearanceRef = ||Tip2_{ine} - PointTower_{ine}|| \tag{3.3}$$

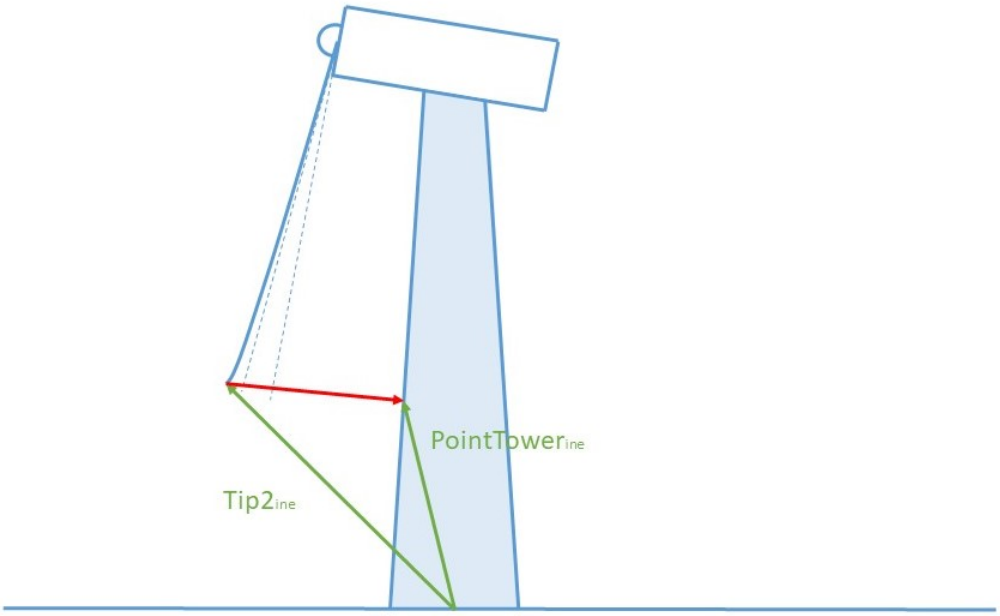

Figure 3.8: Computation of the reference clearance.

Once the reference condition is defined, the next step is to compute the clearance during all the operative conditions and to identify the condition that minimizes it. For each blade, for each DLC and at each time step a sensor measures the relative position of the tip of the blade concerning the initial position.

The clearance for each condition is computed in this way:

$$Clearance(i) = ||Tip(kk)_{ine} + RelatDisp_{ine} - PointTower_{ine}|| \tag{3.4}$$

The condition in which the clearance is minimum is selected and the following information is saved: number of DLC, number of blade, reference time, teeter angle, blade tip displacement, clearance, safety factor, loads, and displacements. All this information is used by the code during the next steps.

The minimum clearance that can be reached during all the possible lifetime conditions is defined by the regulations:

$$MinClearance = ClearanceRef * (1 - SafetyFactor) \tag{3.5}$$

The constraint referred to the minimum clearance is defined as:

$$CTip = \frac{MinClearance - Clearance}{MinClearance} \tag{3.6}$$

The constraint is satisfied if $CTip < 0$, that is when the minimum clearance obtained during the envelope is higher than the reference value. The CTip also gives the information of how much the constraint is satisfied because it is a normalized parameter.

The last step before running the optimization procedure is the definition of the simplified model used for the tip constraint. The model is made by a blade connected to the ground. The main difference concerning the original case are the reference loads used for the first iteration step. A proper initial guess helps the convergence of the method because the loads that act on the rotor deflect the blade and also contribute to the dynamic of the rotor. Therefore, it is necessary to modify the previously saved loads to achieve a proper initial guess used for the optimization.

$$Loads_{intialguess} = Loads_{maxtipdisp} * (1 - sin(TeeterAngle)) \tag{3.7}$$

The loads have been reduced, in function of the teeter angle, with respect to the real condition and are used as starting points to find a set of loads that give a blade deflection as close as possible to the reference condition. An iterative process based on a gradient descend method is used to find the required solution that satisfies the prescribed constraints.

Once the convergence is achieved, the structural optimization process begins. The internal structure of the blade is changed at every iteration and as a consequence, the constraints are computed at every iteration. To verify the clearance, the set of loads previously found are applied to the simplified model, composed of the teeter hinge and the blade, and the tip displacement is computed by the sensors.

It is important to remember that in the simplified model, the reference frame used by the code refers to the blade. As a consequence, to compute the clearance it is necessary to calculate the position of the reference point on the tower in the local reference system. In order to do this, a translation and a set of plane rotations are computed:

$$PointTower_{blade} = ((PointTower_{ine} - BladeRoot_{ine}) * rot_1) * rot_2 \tag{3.8}$$

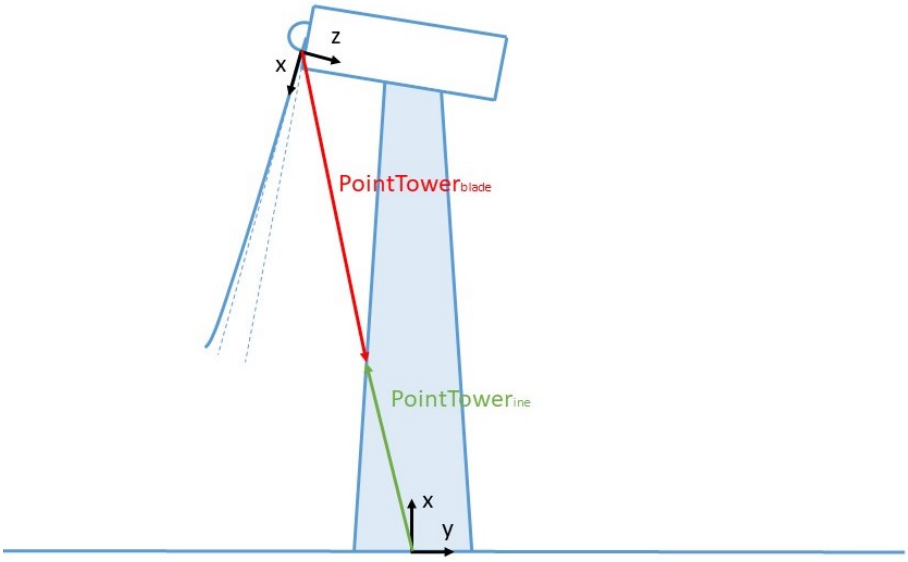

Figure 3.9: Change of reference system.

The first rotation is used to move from the inertial reference to the blade initial reference, the second rotation is to take into account the up-tilt angle, the cone angle, and the reference teeter angle.

After this change of reference system it is possible to compute the clearance:

$$Clearance = ||PointTower_{blade} - TipDispInitial_{blade} - RelDisp_{blade}|| \tag{3.9}$$

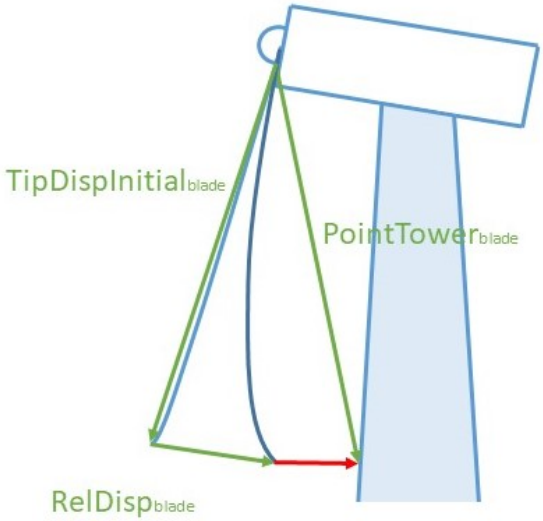

Figure 3.10: Computation of the deformed clearance.

The last step is to compute the constraint, comparing the clearance with the minimum admissible value:

$$CTip = \frac{MinClearance - Clearance}{MinClearance} \tag{3.10}$$

The constraint is satisfied if $CTip < 0$ and the computation is finished. This new procedure, compared with the original one, permits to consider the displacements due to the presence of a non-fixed hub. The displacements due to the movement of the rotor around the teeter hinge can be considerable and decisive in satisfying the clearance. The incorrect identification of the load condition sized for clearance affects the entire structural optimization and does not guarantee compliance with the constraint imposed by the regulations.

All this procedure is implemented in the Cp-Max optimization code and it can be considered more general and usable for all the machines because it uses absolute displacements. In the next chapter 4 a parametric analysis and some considerations related to this important topic are done.

3.3.3 Original vs New method

In table 3.1 a comparison is shown between the two methods usable for the computation of the minimum clearance. The wind turbine studied and the DLC used are the same for both methods. This analysis was performed to highlight the differences in the numerical results between the two procedures.

	Original-procedure	New-procedure
DLC	1.3 11m/s	1.4 minus v_o d
Tip deflection [m]	20.1	3.5
Teeter angle [deg]	0.3	9.1
Clearance [m]	6.6	0.8

Table 3.1: Original vs New procedure for the clearance computation.

The two methods identify different DLC at which different values of clearance are related. The original procedure identifies the condition in which the displacement of the blade is higher, as expected due to the code definition. The teeter angle that corresponds to this condition is close to zero degrees. Therefore the reduction of the clearance due to this angle is much lower than the reduction due to the blade deflection. The clearance that results is close to the minimum admissible value.

The new procedure identifies a complete different condition. In this case the teeter angle is considerable, therefore the reduction of clearance due to this contribution is higher with respect to the reduction due to the blade deflection. The clearance that results is not compatible with the wind turbine constraints because this value is far from the minimum admissible clearance.

In conclusion, the original method identifies correctly the condition of the highest deflection to which, however, the condition of minimum clearance does not comply to. Therefore the design process is compromised because the wind turbine does not satisfy all the constraints. For this reason it was necessary to implement the new procedure for the calculation of the clearance.

Chapter 4

Comparison and Results

4.1 Baseline

As seen in chapter 1 the most common configuration for multi-megawatt wind turbine is the HAWT up-wind configuration with three blades. The baseline case for this work is the 20MW PoliMi wind turbine generated by MATLAB, and originally derived from a 10MW turbine with three blades and up-wind configuration.

Rated power $[MW]$	20.0
IEC class	I C
Number of blades	3
Rotor orientation	Upwind
Control	Variable speed, collective pitch
Drive-train	Single stage
Rated Wind Speed$[m/s]$	11.60
Rated rotor speed$[RPM]$	6.77
Blade length$[m]$	122.14
Rotor diameter [m]	252.20
Hub height$[m]$	167.93
Tower height$[m]$	163.17
Nacelle up-tilt $[deg]$	5.0
Rotor pre-cone $[deg]$	2.5
Cut-in wind speed$[m/s]$	4
Cut-out wind speed$[m/s]$	25
Blade mass $[kg]$	113'505
Total tower mass $[kg]$	630'000
AEP $[MWh]$	97510
CoE $[\$/MWh]$	75.00

Table 4.1: Baseline properties.

This configuration has been used as initial guess to obtain a structural optimized three-bladed turbine, and as initial guess to obtain a two-bladed turbine as well. The main characteristics of the wind turbine are summarized in table 4.1.

The controller used for all the machines analysed in this work has been set by the PoliWind Team and is an LQR controller with the integration term of the rotor velocity. Given the generous size of the turbine and the nominal power involved the use of an LQR controller was preferred to a PID controller.

The states used by the controller are $[d, d_{dot}, Omega, Beta, Beta_{dot}, Torque]$, and the matrices scheduled values used to compute the LQR settings are shown in the following table 4.2:

Tag	Value	Meaning
Winds	[3, 9, 14, 30]	Values of wind speed
$Weights_Q$	$[0, 0, 1, 0, 0, 0]$	Weights on the state
$Weights_{RBeta}$	$[1, 1, 0.1, 0.1]$	Weights on the controls: Beta
$Weights_{RTel}$	$[0.1, 0.1, 0.1, 0.1]$	Weights on the controls: Torque
$Weights_{QIntegral}$	$[0.01, 0.1, 0.1, 0.1]$	Weights on the Integral term of the state

Table 4.2: Setting of the LQR controller.

The internal configuration of the blade is standard, as described in chapter 2, with the addition of a third shear web due to the large size of the blade. This arrangement will be the same for all the cases analysed in this work, whereas the thicknesses of the various components to be optimized by Cp-Max will be different. The positions of the components are shown in figure 4.1.

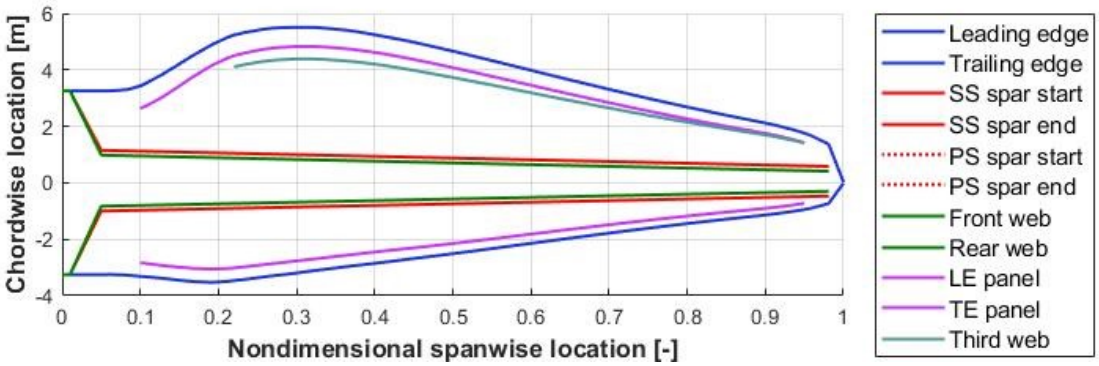

Figure 4.1: Blade structure.

4.2 Solidity Analysis

As already mentioned in chapter 3, in this project the design of the two-bladed wind turbine uses as initial guess a three-bladed turbine from which a blade is then removed. After this operation, it is necessary to adopt some modifications to the model because the procedure of blade removal reduces significantly the solidity of the rotor and consequently provides low performance, the most relevant being the reduction of the AEP. It must be noticed that the solidity represents the area occupied by the blades concerning the total rotor disk area.

Therefore, as seen in figure 4.2, the main parameters that need to be modified, moving from a three-bladed to a two-bladed turbine, are the blade chord distribution and consequently the blade thickness of the profiles.

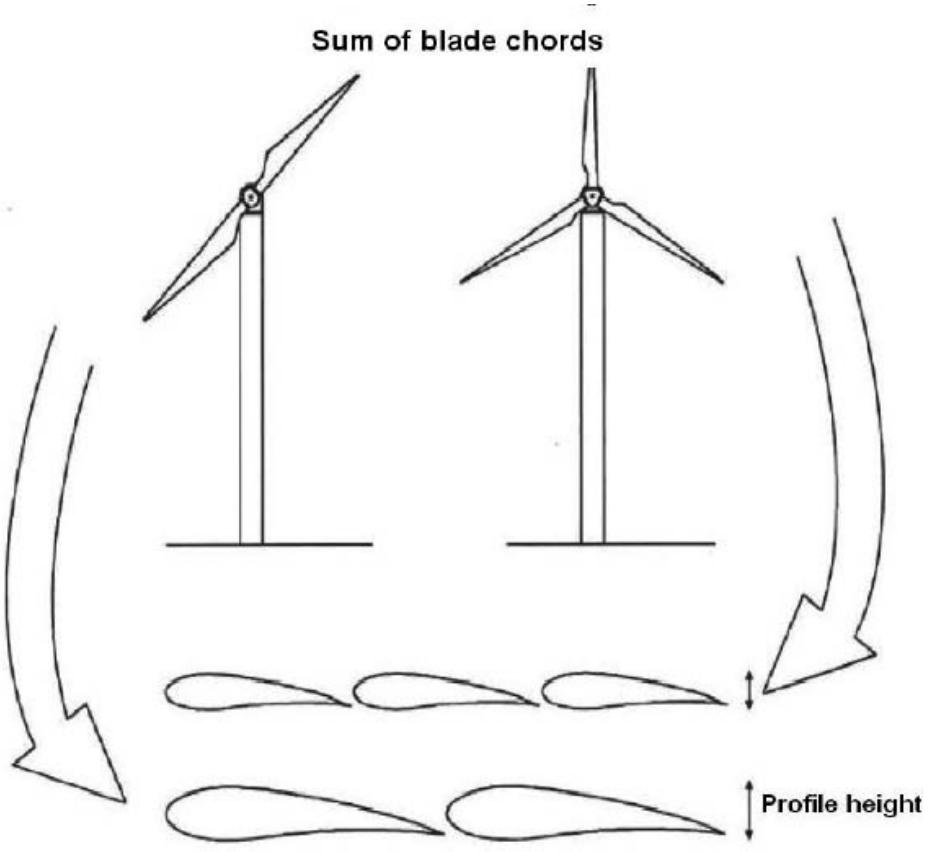

Figure 4.2: Chord and thickness variation [17].

The rotor solidity in Cp-Max is one of the macro variables because it greatly affects the design and the operation conditions of the rotor, and as a consequence, it is frozen at each global iteration. For example, a decrease of the solidity generates an increase of the optimum TSR and an increase of the corresponding Ω. As a result, the trajectory regulation changes and consequently the power curve as well.

Therefore, it is necessary to understand how to modify the blade for a two-bladed turbine, starting from a three-bladed turbine geometry, changing the solidity value of the rotor. The increase of the solidity increases the mass of the single blade but the removal of one of the three blades reduces the mass of the rotor and so the ICC. Consequently, it is necessary to find the best compromise between costs, loads generated, and energy

production.

The chord distribution must be changed in order to change the solidity. There are unlimited ways to change the chord distribution depending on the design constraints, generally defined by manufacturing process limits or other design constraints. Civati in his work [13] analysed the solidity variation for a two-bladed 10MW turbine in two different ways. Starting from his work, a preliminary analysis has been done.

It has been decided to adopt a simple strategy without upper limits on the chord maximum value and on the root diameter. The increase of the chord value is made linearly along the blade, following a growth of 2% solidity at time, up to +20% as it is seen in figure 4.3.

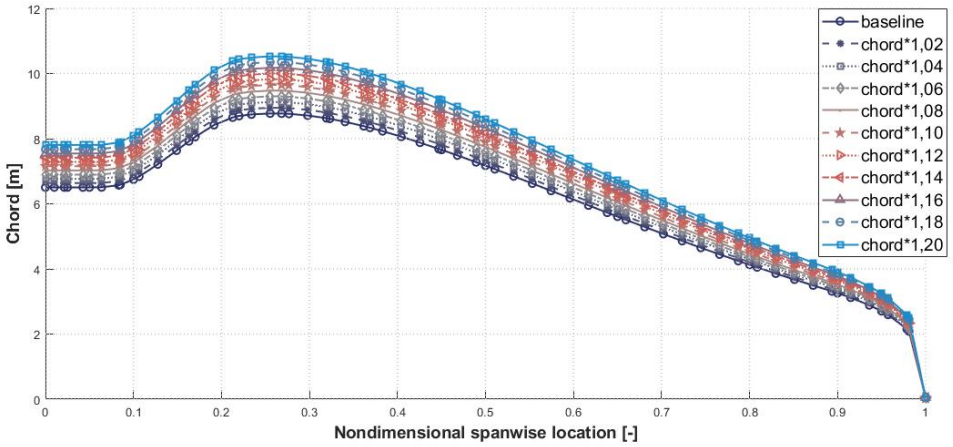

Figure 4.3: Chord distribution variation.

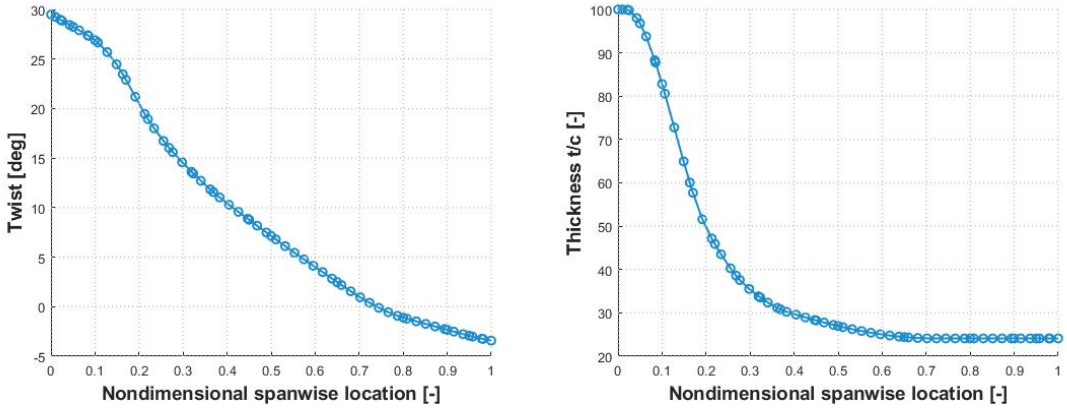

Figure 4.4: Twist and thickness distribution.

A complete aerodynamic optimization has not been performed, firstly as it is not the main focus of the work and secondly for a matter of computational time. Therefore, the airfoil types, their positions along the blade length, the twist distribution, and the sweep distribution have not been modified, as can be seen in figure 4.4.

Chord	ΔAEP[%]	$\Delta Mass$[%]
2B baseline	-	-
102%	+0.029	+1.048
104%	+0.052	+2.096
106%	+0.071	+3.144
108%	+0.086	+4.192
110%	+0.099	+5.240
112%	+0.111	+6.297
114%	+0.120	+7.353
116%	+0.128	+8.401
118%	+0.133	+9.799
120%	+0.137	+10.515

Table 4.3: Blade mass and AEP variation.

The analysis was computed through the static performance evaluation, thus estimating the turbine performance without considering the DLC1.1 to estimate the AEP. This was decided because the goal of this analysis is to understand in first approximation a suitable growing chord value yet with a reasonable computational time. The results shown in table 4.3 highlight that the AEP grows as solidity increases, as expected. On the contrary if solidity increases, also the blade mass increases at each iteration and accordingly do the costs.

The CoE was not computed because, to be appropriate, a complete design and a the turbulent AEP are needed and also because the resulting configurations are not optimized. In addition, with reference to the work of Civati [13] the selected configuration is the one which has a solidity increased by 18% as a compromise between the AEP and mass increase. The external geometry obtained is used for all the two-bladed configurations analysed in the next sections.

4.3 Parametric Analysis

As already mentioned in chapter 3, the clearance for a two-bladed turbine of this magnitude is a sensitive issue due to the presence of the teeter hinge. Therefore, it could be useful to know how some global parameters affect the clearance and the CoE after an optimization process.

In this paragraph, a parametric analysis is performed changing the up-tilt angle and the stiffness of the teeter hinge to highlight how they affect the design process, the costs, and the clearance. These two parameters have been selected because they are predominant in affecting the clearance and because they can be changed without disrupting the machine. The other parameters that affect the clearance are the rotor overhang and the pre-cone angle, but it has been decided to freeze them.

The design of a wind turbine is very complex because the variables involved are numerous and the effects of their changes reflect on several aspects. Ideally, provided that the Cp-Max code optimizes the entire machine by activating all the variables, the result will be a configuration that minimises the cost of energy. As a matter of fact, this is not possible because the calculation times are extremely long due to multiple variables. Therefore, for the design of a real machine, the majority of the parameters are defined and a small set of variables are included in the optimization process, also considering the possibility of manufacturing the components.

The idea of this analysis is to start from the three-bladed turbine blade structure, change only the solidity value (according to the last section 4.2), give a prebend to the blade, and use as initial guess of the teeter stiffness the one represented in figure 3.4. The next step is the identification of the load condition that maximizes the deflection of the teeter hinge. From this point, the stiffness of the teeter hinge [34] is designed to reduce the maximum rotor plane rotation. The last step is the selection of a set of configurations of up-tilt and stiffness that have to be run by the structural optimizer.

4.3.1 Geometry and identification of the problem

It was decided to give the blade a prebend firstly to maximize the energy captured in the operative conditions, and secondly to promote the satisfaction of the tip displacement constraint by increasing the distance between the blade and the tower. The prebend distribution results from the prebend design submodule. A maximum tip value of 6m was set to comply with the previous work [20], and the resulting distribution is shown in figure 4.5.

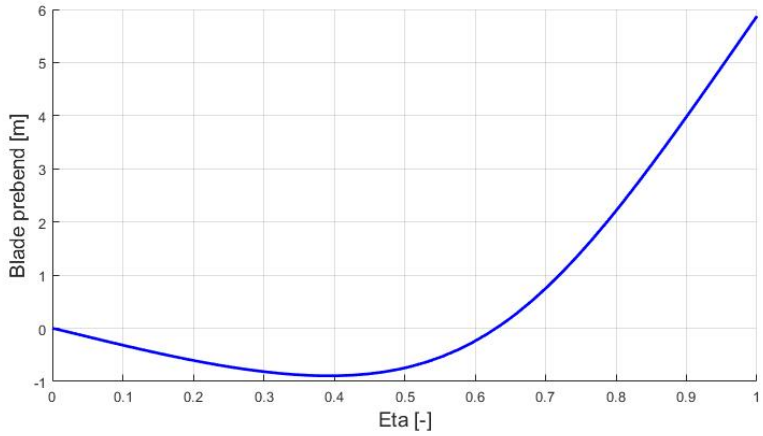

Figure 4.5: Prebend distribution.

The prebend will also allow for a lighter and consequently less expensive blade. The blade external geometry is fixed and the main geometry parameters of the machine that influence the clearance are shown in table 4.4.

Tower height [m]	163.2
Hub height [m]	167.9
Rotor overhang [m]	10.0
Tip prebend [m]	6
Blade length [m]	122.1
Rotor diameter [m]	252.2
Up-tilt angle [deg]	5.0
Precone angle [deg]	2.5

Table 4.4: Geometry of the machine.

The undeformed clearance that results is $27.02m$. The teeter hinge considered allows the rotor to oscillate between $-11deg$ and $+11deg$. The definition of this interval derives from a previous study carried out on a two-blade turbine with a power of 3MW. This setting is not compatible with this 20MW two-bladed because solely the rotation of the teeter hinge of 11deg reduces the clearance to $3.6m$ and does not satisfy the minimum clearance allowed, which according to the regulations (for the operative conditions) is 30% of the undeformed clearance. It is possible to see in table 4.5 how the clearance changes only to the effect of the variation of the teeter angle.

Teeter angle [deg]	Clearance [m]
0	27.02
5	16.39
7	12.12
9	7.87
11	3.60

Table 4.5: Clearance variation in function of the teeter angle.

4.3.2 Teeter hinge design

Therefore, it is necessary to reduce the maximum oscillation and correctly design the stiffness of the teeter hinge. The following step is the identification of the load case that maximizes the teeter hinge deflection, following an iterative analysis to identify a stiffness setting that reduces the oscillation of the rotor between $-5deg$ and $+5deg$. The result could be a good compromise between a significant reduction of the maximum teeter angle and a too stiff teetering hub that cannot absorb loads.

The DLC in which the teeter hinge deflects more is the 1.4 families. The specified one is the "1.4 minus v_o d" representing an extreme wind change of direction at the cut-out velocity. The strong oscillations occur when the machine is turned off by the control system because an aerodynamic counter torque is used to slow down the rotor. The trend of the teeter angle is shown in figure 4.6.

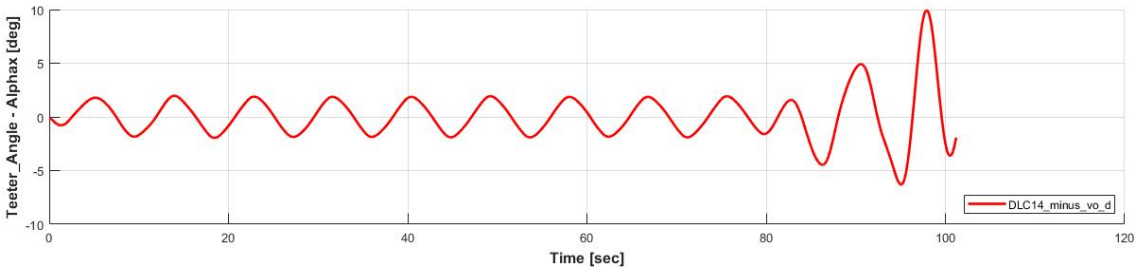

Figure 4.6: Teeter angle trend during the DLC 1.4 v_o d.

All the four cases of "1.4 minus v_o" are used to determine the new stiffness properties. The spring constant was increased by various percentages and for each case, the DLC were performed. In table 4.6 it is possible to see the various tested settings.

Stiffness	Maximum oscillation [deg]
$1.8 * 10^7 Nm/deg$	9.9
+20%	8.3
+50%	6.1
+60%	5.5
+70%	4.9

Table 4.6: Deflection of the teeter angle with respect to the spring stiffness.

Starting from the results of this analysis it is reasonable to select two stiffness configurations, respectively one incremented by 60%, called configuration A, and the other incremented by 70%, called configuration B, given that at maximum angle deflection they admit a maximum deflection to the blade of about $10m$. These choices were made considering that the maximum blade deflection and the maximum angle oscillation of all the load cases usually do not happen at the same time. This is reasonable and corresponds to the real operative conditions that the turbine will encounter during its operational life.

The new teeter hinge characteristics are shown in figure 4.7 and in figure 4.8.

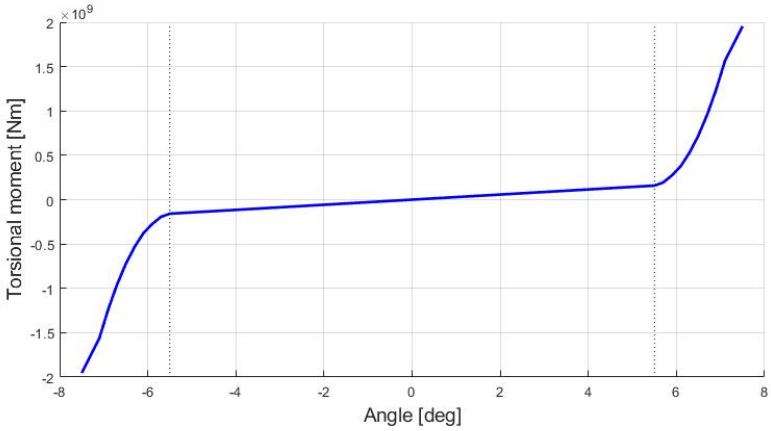

Figure 4.7: Teeter spring with linear constant $= 2.9 * 10^7 Nm/deg$. Configuration A.

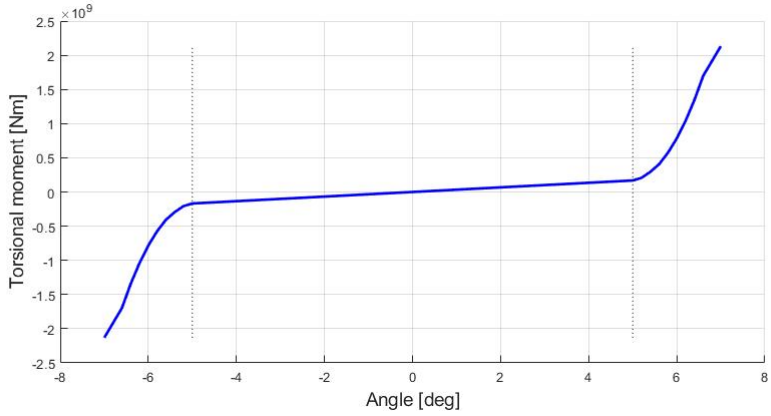

Figure 4.8: Teeter spring with linear constant $= 3.4 * 10^7 Nm/deg$. Configuration B.

At this point the teeter hinge is well sized in two possible configurations. The next step is the verification with all the DLC of these two choices, bearing in mind that the dimension process has been performed only with the DLC that stress more the teeter angle. Now it is time to define some reasonable configurations for the parametric analysis from which useful information for our analysis can be obtained. In the following table 4.7 there is a summary of the combination of stiffness of the teeter hinge and up-tilt angles.

Stiffness configuration	Up-til [deg]
A	5
A	7
B	5
B	7

Table 4.7: Combination of stiffness and up-tilt angle.

The purpose of a higher value of the up-tilt is to achieve a bigger clearance, and as a consequence a lighter blade. The most important disadvantage is a reduction of the

energy captured because of the relative angle between the rotor plane and the wind velocity. However, an up-tilt angle is necessary for an upwind machine, especially of this magnitude.

Generally, the response of the turbine will change for every configuration and this analysis has the goal of understanding how it affects the structure of the blade and the energy captured. The best solution is the one that minimizes the cost of the energy and that satisfies all the constraints.

4.3.3 Configurations and results

The configurations used for the analysis combine the selected up-tilt angles (5deg, 7deg) with the two stiffness configurations of the teeter hinge. The following tables (4.8 4.9 4.10 4.11) show the main results of the different configurations in terms of constraints and CoE.

Blade mass [kg]	113800
CoE [$/MWh]	85.43
Constraint on blade frequency [%]	55.56
Constraint on flap-edge freq.ratio [%]	17.62
Constraint on clearance [%]	0.01

Table 4.8: Stiffness A & Up-tilt 5deg.

Blade mass [kg]	115300
CoE [$/MWh]	85.51
Constraint on blade frequency [%]	55.82
Constraint on flap-edge freq.ratio [%]	17.95
Constraint on clearance [%]	0.32

Table 4.9: Stiffness B & Up-tilt 5deg.

Blade mass [kg]	109600
CoE [$/MWh]	86.39
Constraint on blade frequency [%]	65.30
Constraint on flap-edge freq.ratio [%]	26.54
Constraint on clearance [%]	8.35

Table 4.10: Stiffness A & Up-tilt 7deg.

Blade mass [kg]	110000
CoE [$/MWh]	86.38
Constraint on blade frequency [%]	65.65
Constraint on flap-edge freq.ratio [%]	26.54
Constraint on clearance [%]	9.07

Table 4.11: Stiffness B & Up-tilt 7deg.

The configurations presented were obtained using the Cp-Max structural optimization module suitably updated and modified to support the two-blade turbines. The configurations are comparable as they all respect the constraints and in addition the structural cycles converge in all cases.

The new teeter hinge configurations allow for case A a maximum deflection of 5.5deg and for case B of 5deg. This means that the dimensioning load condition for tip displacement for both configurations is no longer the DLC 1.4. It must be considered that the clearance between the blade and the tower for a two-bladed turbine depends on the combination of the displacement given by the teeter angle and the one given by the deformation of the blade. In the load case 1.4 the teeter deflection is high but the blade deflection is minimal, so after the limitation of the excursion of the teeter hinge, the condition of minimum clearance has changed. The condition in which the clearance is minimum results from the 1.3 families, an operating condition with strong turbulence and in which the teeter angle is limited while the deflection of the blade is emphasized. Therefore, due to the stiffness of the teeter increased with the previous analysis, the deflection of the blade appears to be dominant in the calculation of the constraint in the design of the turbine.

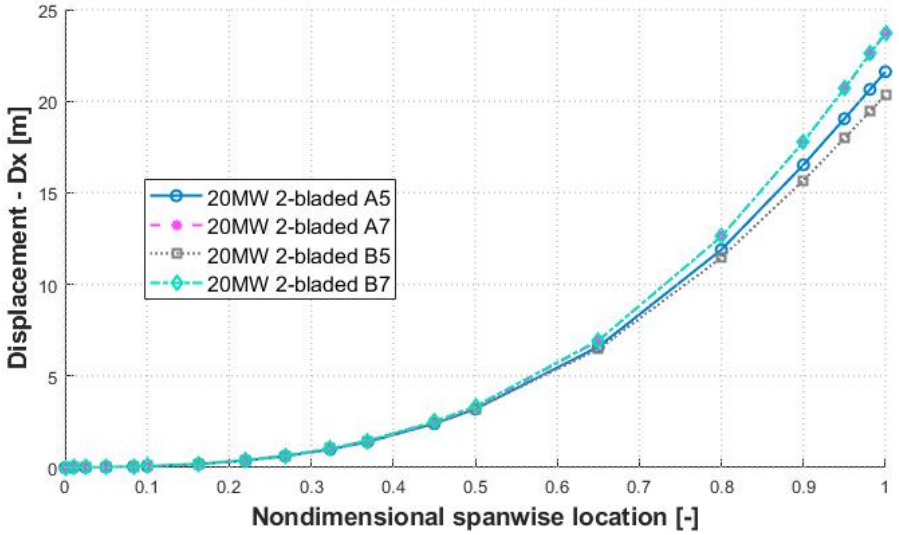

Figure 4.9: Tip displacement and clearance.

The results from the different configurations are shown in figure 4.9. The configurations with the largest up-tilt have a higher clearance and as a consequence, if the same teeter angle occurs, the blade can deflect more. On the other hand, with the same blade deflection, the teeter angle can be higher.

Analyzing the data of the various configurations, the machines with an up-tilt angle of 5deg have the tip displacement as active constraint, while the other configurations seem not to have an active constraint. This is due to the optimization process because the blade initial guess for all the configurations was optimized for 5deg of up-tilt, consequently a few optimization cycles were not enough to find a solution with the constraint of tip displacement active. The other constraints involved that affected the optimization of some sections of some components are strain, stress and fatigue.

Another significant result from the analysis of the data is that the frequency con-

straints are largely satisfied. This is slightly due to the increase in the distribution of the chord and mainly to the initial blade guess being a three-bladed. The structure and the limits for the design thicknesses have not been distorted, consequently the main reason of this result is the comparison of the first flapping frequency with the 2P rather than the 3P. In figure 4.10 it is possible to see the frequency of the first and second eigs of the blade, that strongly depends on the thickness of the internal components. For this reason, configurations with the same up-tilt are similar.

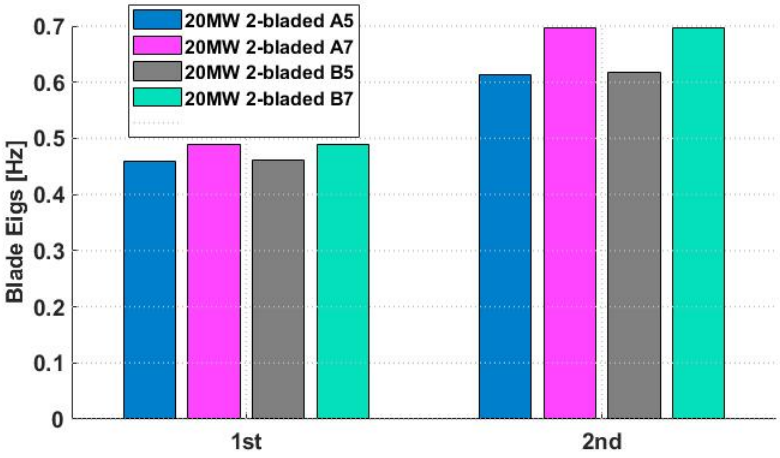

Figure 4.10: Eigs.

It is observed that the CoE between the various configurations changes slightly and in first analysis does not give an indication on which configuration could be the best. This is because as already noticed in chapter 2, the cost model used for this 2-bladed 20MW is not verified but used only as indicator between similar configurations.

In figure 4.11 the configuration A5 is compared with the other three configurations in terms of mass, AEP and CoE. The AEP is higher for the configurations with 5deg of up-tilt, as expected, because it largely depends on the angle between the rotor plane and the horizontal wind main direction. The mass of the blade is lower for the two configurations with 7deg of up-tilt because the clearance in these cases is higher so it is possible to have a more flexible and lighter blade. Lastly, the CoE values show that in these cases the reduction of mass is not rewarded, as it also implies a reduction of AEP. The result is that the configurations with 5deg of up-tilt are slightly convenient with respect to the others.

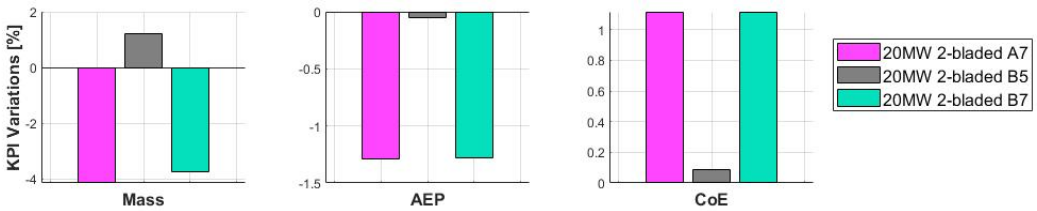

Figure 4.11: Mass, AEP and CoE comparison.

Therefore, it is necessary to proceed considering other parameters, limited not only to the value of the energy cost, but with reference to the ultimate loads and fatigue DEL. In the following figures 4.12 4.13 4.14 the main significant loads indicator are shown for the four different configurations, normalized to the A5 machine.

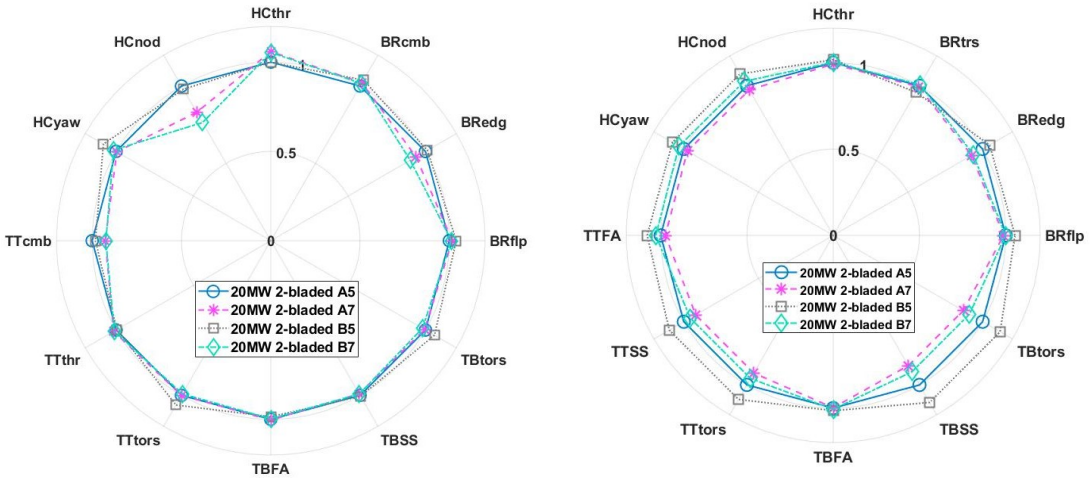

Figure 4.12: Ultimate loads and fatigue DEL comparison.

Most of the ultimate load indicators turn out to be very similar for all the configurations, except for a reduction of the BRedg (blade root edgewise moment), the TTcmb (tower top combined moment), and the HCcomb (hub center combined moment) for the 7deg up-tilt configurations. This is due probably to a better compromise resulting from the interaction between the stiffness of the blade and the rotor oscillations.

Examining the DEL, it is possible to highlight that in the configurations with an up-tilt of 7deg most of the moments are lower than in the 5deg configurations. In addition, the stiffer configuration of the teeter hinge (B) has higher DEL indicators.

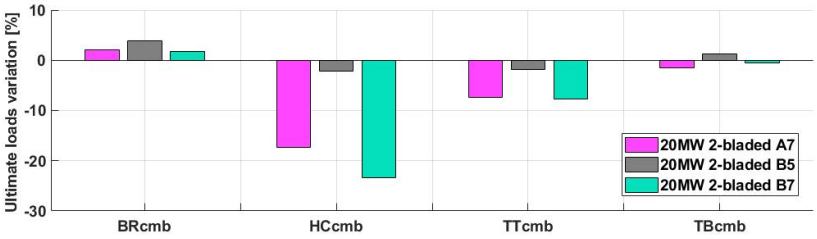

Figure 4.13: Ultimate loads summary comparison.

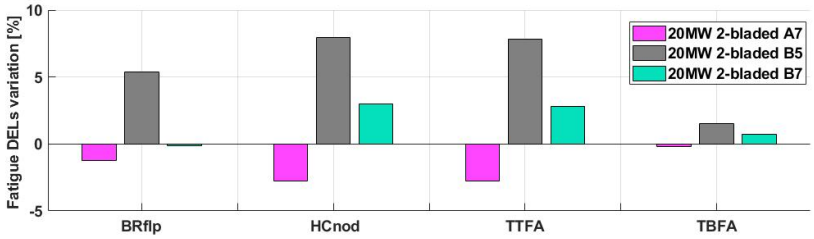

Figure 4.14: Fatigue DEL summary comparison.

4.4 Comparison with three bladed

In this last section, a brief comparison was performed between a two-bladed configuration, the A5 of the previous section 4.3, and a three-bladed configuration. A structural optimization has also been run for the three-bladed in order to have two optimized configurations to compare. The differences in terms of static performance, power curves, constraints and loads are analysed to highlight the advantages and disadvantages of the two configurations.

4.4.1 Geometry and tip displacement

For both configurations the prebend submodule has been run with the goal of optimizing the energy captured by the rotor. The two prebend distributions are different, as seen in figure 4.15, due to the different chord distribution that implies different stiffness and aerodynamics properties for the two structures.

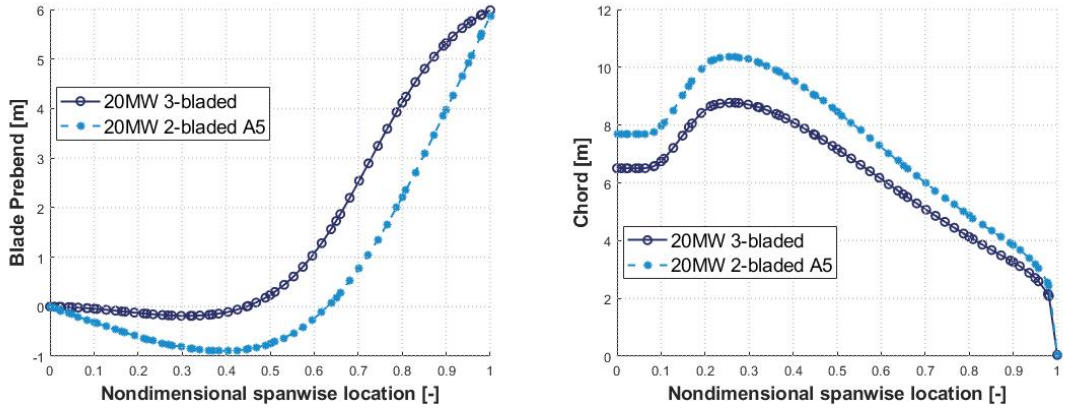

Figure 4.15: Prebend and chord distribution.

The maximum tip-displacement that results is very similar because the undeformed clearance is the same and the load case in which it results is also the same (DLC1.3 11m/s). The less displacement for the two-bladed configuration is due to the teeter angle deflection that slightly reduces the displacement of the blade. The teeter angle in this case is less than 1deg, which justifies the small differences with respect to the three-bladed.

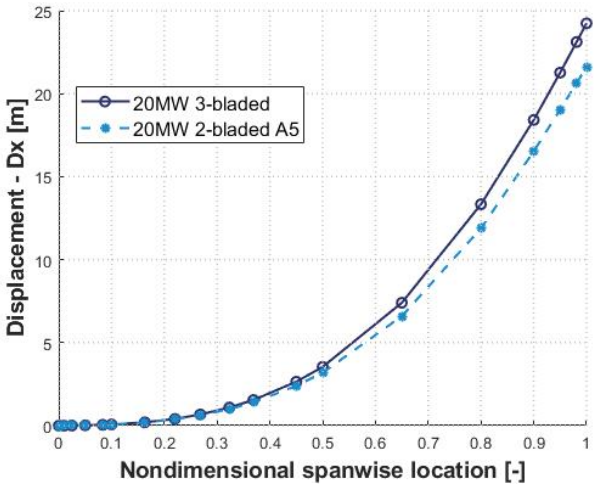

Figure 4.16: Tip displacement comparison.

4.4.2 Blade root loads and structural elements

In the following images 4.17 4.18 a comparison between the blade root moments is presented. It can be noticed that the flap-wise and edge-wise bending moments are higher in the two-bladed configuration, implying a higher combined flap/edge bending moment. These loads occur during operative conditions, DLC1.3 and DLC1.4, when the blades are greatly stressed, in the first condition because of the high turbulence and in the second condition because of the extreme change of direction. This result is expected due to the better balancing of the three-bladed rotor. Concerning the torsional moment, it is largely higher on the two bladed-configuration but it is not a dimensional moment and for this preliminary analysis it has not been investigated.

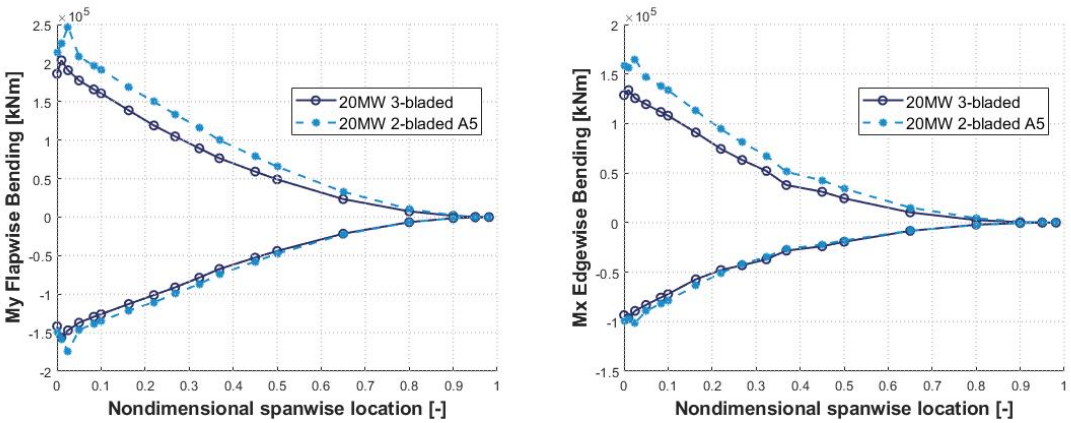

Figure 4.17: Flapwise and edgewise blade root bending moment.

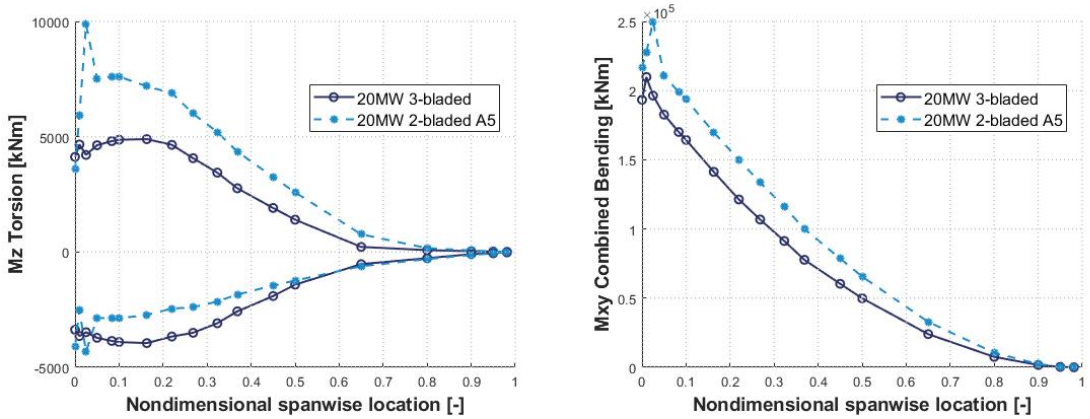

Figure 4.18: Torsional and combined blade root moment.

The thickness of all the structural components is shown in figure 4.19. The distributions result from the structural design submodule, which tries to optimize each element thickness by minimizing the ICC and satisfying all the constraints.

The main differences between the two-configurations are due to the different loads that act on the structures. It was noticed that the chord distribution is different and this implies different stiffness properties of the two structures only by looking at the external geometry.

The three-bladed configuration is a machine studied previously and optimized aerodynamically and structurally in former works. The two-bladed configuration is not aerodynamically optimized and in this preliminary design the external geometry was frozen in order to optimize the internal structure. The resulting thickness distribution obviously allows the blade to satisfy all the constraints but does not represent an overall optimal solution for sure. The first reason is that the initial guess configuration and the bounds in an optimization process largely influence the quality of the results and the second is that not all the parameters were activated for the optimization process due to the computational time required. This is the reason for the strange thickness picks that occur in some elements.

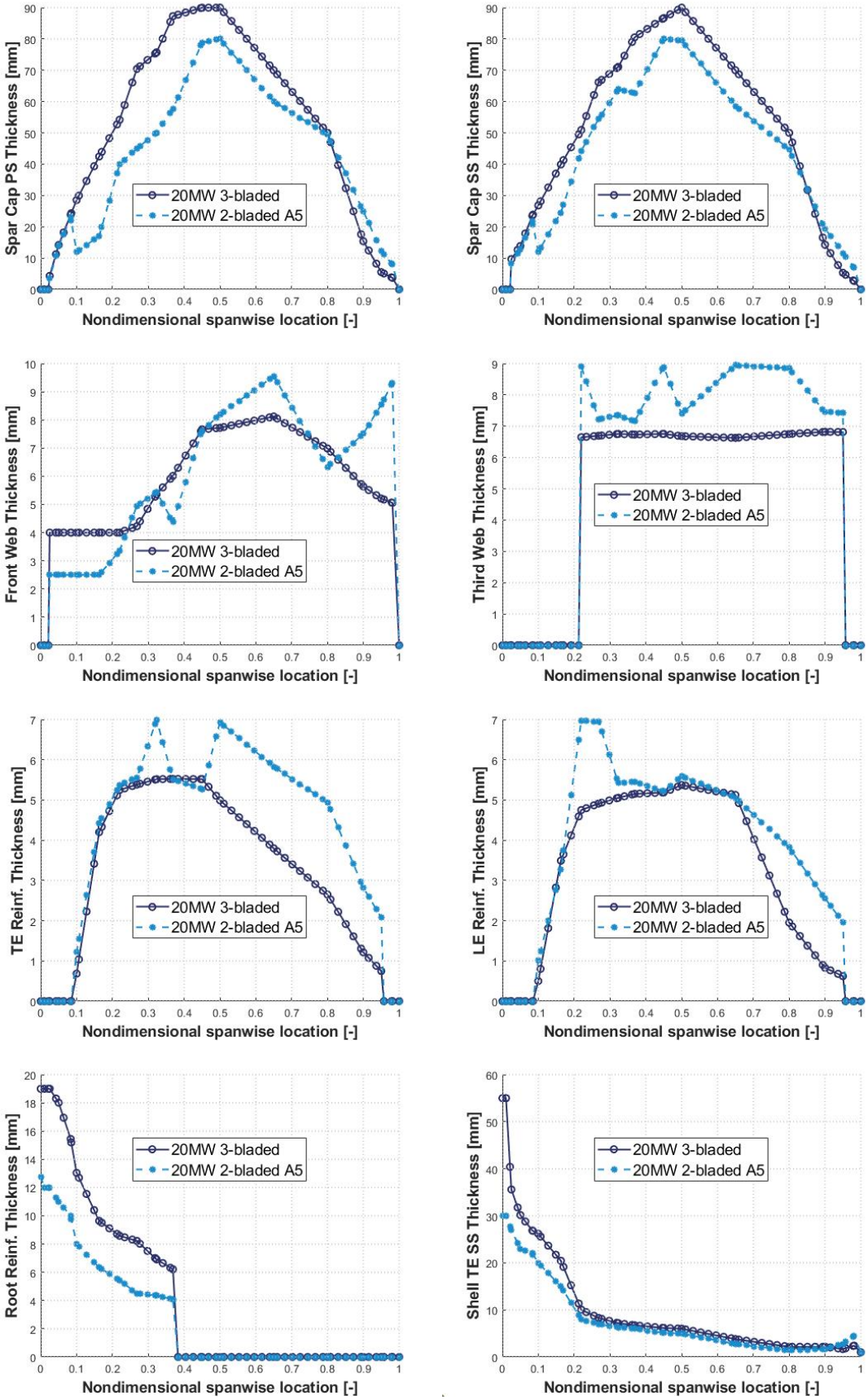

Figure 4.19: Structural elements thickness.

4.4.3 Ultimate and fatigue Loads

The following figures 4.20 4.21 show a summary of the most significant loads that act on a wind turbine. In both the representations the loads of the two-bladed configuration are compared to the normalized three-bladed solution.

The first figure 4.20 shows the ultimate loads that act on the blade, on the tower, and on the hub. It can be noticed that the loads resulting on the three-bladed configuration are lower that the two-bladed. The highest differences result on the tower base side/side bending, on the tower top combined bending and on the hub centre nodding.

The high loads that act on the tower come out from both configurations from the DLC1.4 v_o, in which there is an extreme change of wind direction at the cut out velocity that implies a shutdown of the machine. During this phase, the aerodynamic force generated on the blade is used to slow down the rotor speed, stressing the teeter hinge that oscillates greatly and transmits the loads on the tower. In this preliminary work the controller settings were not changed. A proper design of the controller could be helpful to reduce the high loads generated, for example by lowering the pitch rate during the shutdown process.

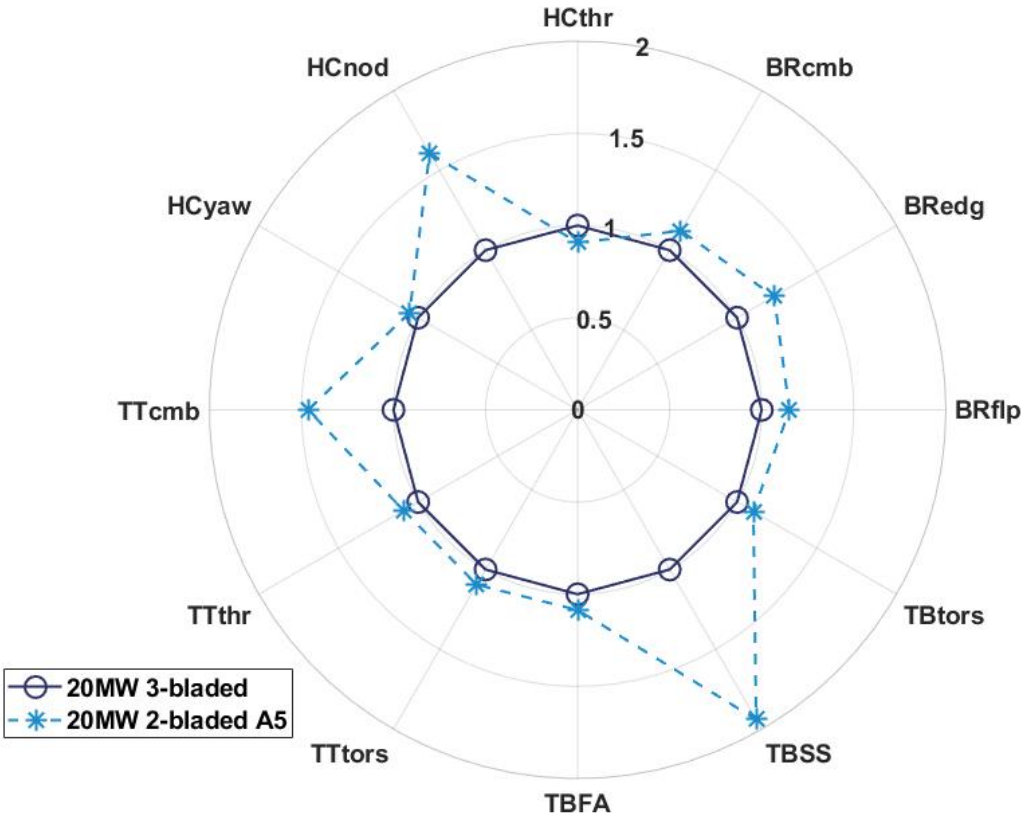

Figure 4.20: Ultimate loads summary comparison.

The second figure 4.20 shows the fatigue DEL that acts on the blade, on the tower, and on the hub. This summary points out that the tower is the part of the structure most subjected to fatigue loads. Looking at figure 4.22 it is highlighted that at low wind speed, from 7 to 11 m/s, the picks are largely higher with respect to the three-bladed

configuration. This could be due to the teeter hinge properties that allow to mitigate higher loads in the tower with respect to a two-bladed configuration without a teeter hinge. However, the high stiffness, which has to ensure a maximum limited deflection, still unloads considerable loads on the tower. This gives much higher oscillations and as a consequence higher DEL.

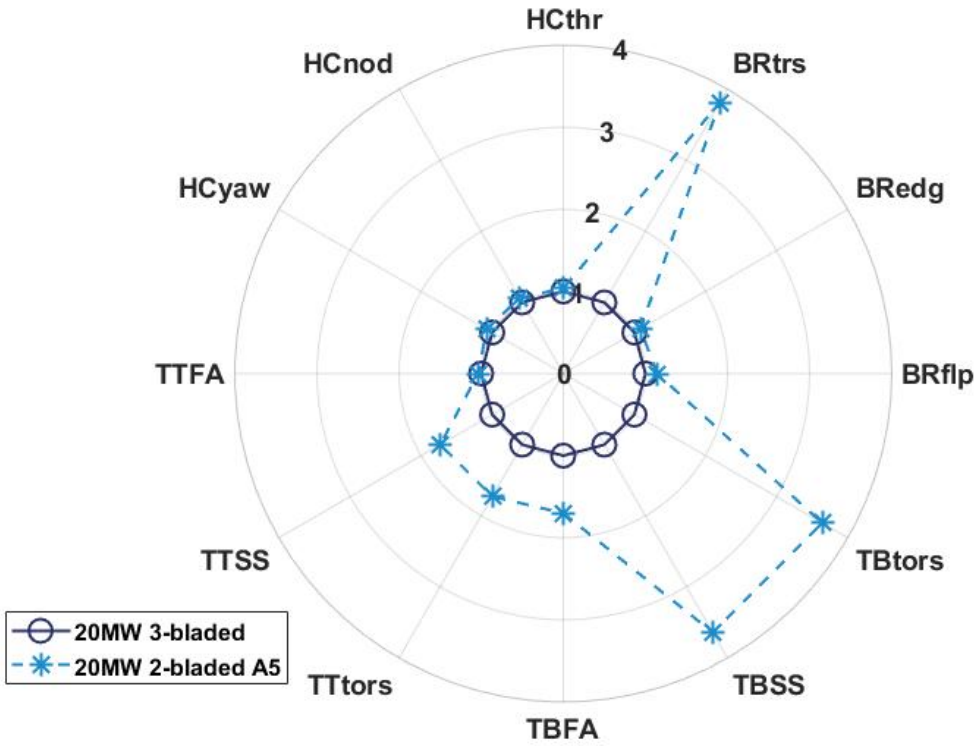

Figure 4.21: Fatigue DEL summary comparison.

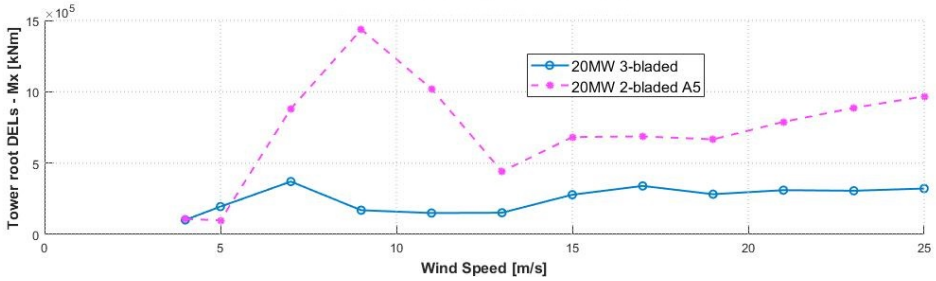

Figure 4.22: DEL vs wind, tower base side/side comparison.

4.4.4 KPIs and constraints

The most important KPIs of a wind turbine design are the CoE and the AEP. These two parameters alone reveal the integrity of a project in terms of costs and energy production. They are also useful indicators when it is necessary to compare two machines at the first level.

	3-bladed	2-bladed A5
CoE [$/MWh]	85.31	85.44
AEP [GWh/yr]	91.50	89.41

Table 4.12: CoE and AEP comparison between three-bladed and two-bladed.

The three-bladed configuration has a higher power coefficient, therefore the energy captured is higher with respect to the two-bladed configuration. The lower energy captured is compensated by the main advantage of this configuration, which is having one fewer blade and this reflects on the lower cost of the turbine. The CoE that result are very similar, but it must be taken into account that the cost model used is the same for both configurations and it is not optimized for either machines, as specific cost models for 20MW turbines have not yet been implemented in the code.

This is the reason that these reference numbers have to be used only for overall considerations. In addition, it is necessary to look at other KPIs, such as the constraints and the loads, to better understand how good the two projects are.

The satisfaction of the constraints is mandatory and required for the design of a wind turbine, therefore both the configurations satisfy the required constraint, already defined in chapter 3.

	3-bladed	2-bladed A5
Constraint on blade frequency [%]	2.31	55.56
Constraint on flap-edge freq.ratio [%]	11.87	17.62
Constraint on clearance [%]	0.86	0.01
Max constraint on stress [%]	12.00	0.45
Max constraint on strain [%]	3.39	0.01
Max constraint on fatigue [%]	3.30	0.24

Table 4.13: Constraints comparison between three-bladed and two-bladed.

The three-bladed configuration has two active constraints, the clearance and the constraint on the first flap-wise frequency, while the two-bladed has only one active constraint, the tip displacement. This is because the reference frequency to compare with the first flap-wise frequency depends on the number of blades. Therefore, the reduction from 3P to 2P increases the satisfaction of this constraint, also because the first flap-wise frequency does not change to a great extent between the two configurations (0.453Hz vs 0.459Hz).

The two-bladed configuration has some components designed with respect to the stress and strain constraints. Looking at the data for example, the shear webs thickness in the central sections has been designed with respect to the maximum admissible stress, while the root reinforcement has been designed considering the strain loads.

Chapter 5

Conclusions

In this work, the Cp-Max multidisciplinary optimization software, based on Cp-Lambda, was modified allowing the code to deal with two-blade turbine models. One blade was removed from the three-blade model and then a teeter hinge was added connecting the rotor to the hub. The hinge allows the rotor to oscillate around its plane thus reducing the loads transferred to the hub and the tower. Afterward, it was necessary to identify the azimuth angle at which the static analyses gives the most reliable result. The last but most important modification concerned the computation of the clearance between the tower and the blade constraint. It was essential to update the computation procedure as the teeter hinge allows the rotor to oscillate around its axis and consequently the blade to approach the tower. The clearance for two-bladed turbines is the sum of the deflection of the blade and the displacement due to the teeter angle. After these modifications, Cp-Lambda is able to deal with two-bladed turbines and the optimization modules were used to design the machine in the next steps.

The second part of the work concerned a step-by-step design of a two-bladed 20MW upwind wind turbine. The first step was the modification of the external shape of the blade: this was achieved by changing the solidity value to reduce the loss of energy captured after removing a blade. It was found that an increase in the chord of 18% is a good compromise between increasing the AEP, to compensate for the removal of a blade, and an increase of the mass.

The following step was the sizing of the stiffness of the teeter hinge. It was found that the most critical condition was due to the DLC family 1.4 at the cut-out velocity. Therefore, it was analyzed how the clearance between the tip of the blade and the tower changes in function of the teeter hinge angle, finding that a configuration with a deflection of 5deg is a better compromise between the stiffness value and the remaining clearance. This allows the blade to deflect at the teeter maximum angle and to transfer fewer loads to the tower compared to a configuration without teetering hinge. Consequently, an analysis was performed by changing the stiffness value and selecting two suitable configurations. Then a parametric analysis was conducted comparing four different combinations of up-tilt and stiffness of the teeter. For each one of these combinations an optimization with the structural submodule of Cp-Max was performed. The combinations have 5deg or 7deg up-tilt angle and a stiffness of the teeter hinge that admits a maximum angle of 5deg or 5.5deg. From the comparison emerge four configurations, very similar to each other but in which the changes are highlighted. The resulting four configurations, even though they seem very similar, have different performance.

The 7deg up-tilt configurations adopt a lighter blade because the admissible clearance is higher and as a consequence, the blade deflection could be higher; this implies a reduction of the ultimate hub centre combined moments and of the tower-top combined moments. However, they have the disadvantage of a lower AEP value due to the higher up-tilt angle with respect to the 5deg up-tilt configurations. The lower stiffness configurations have the advantage of reducing significantly the fatigue DEL and slightly the ultimate loads, due to the fact that the oscillations are less opposed by the spring. These configurations also result in a lighter blade giving a lower CoE estimation.

In conclusion of this analysis, the best stiffness teeter configuration is the softest one (configuration A) because it is a good compromise between a rigid hub and a too soft teeter. Concerning the up-tilt angle, the 5deg configuration gives advantages in terms of AEP, and the 7deg configuration offers advantages in terms of mass, ultimate loads, and fatigue DEL on the tower.

Finally, a preliminary comparison was made between a two-bladed and a three-blade configuration. The A5 configuration from the previous analysis was selected for the two-bladed turbine and a structural optimized solution derived from the baseline was selected for the three-bladed turbine. This comparison highlights that in this case it is not possible to look only at the AEP and the CoE , as it gives very similar values because the CoE comes out from the same cost model not optimized for these two machines. For this reason, it is necessary to look also at other parameters to highlight the advantages and disadvantages of the two configurations. Form the constraints comparison, both the configurations result to have the tip displacement as an active constraint. The three-bladed machine has also the first flap-wise frequency as an active constraint while the two-bladed, due to the higher loads, has the strain, stress, and fatigue on some components as active constraints. This highlights that the three-bladed machine is better optimized especially with reference to the external geometry of the blade, but aerodynamic was not the focus of this work. Lastly, looking at the loads that act on the components of the turbine, both the ultimate and fatigue DEL generated are higher on the two-bladed. This occurs especially on the tower because of the architecture of the machine that, in some conditions, oscillates considerably.

However, there is still much work to be done on these types of turbines. This a demanding task, not only due to the two-bladed configuration but also to the high power of the machine, which represents a challenge also for the three-bladed standard configurations. A proper evaluation of the cost of energy specific for these machines with a teeter hinge, a complete design of the blade, and a structural sizing of the tower will highlight the possible advantages of the two-bladed configuration turbine.

5.1 Future Developments

The main limitations in this design optimization work have been the high computational time and the high complexity of the problems. Because of this, analyses were carried out concerning a limited number of components and variables of the wind turbine. Several future developments can be implemented to optimize rotor, tower, or other wind turbine parts, while maintaining the aim of reducing the cost of energy and discovering and understanding the advantages of the two-bladed multi-megawatt wind turbines.

- Design of the blade: during this preliminary work a blade from a three-bladed configuration has been used as starting point. The macrostructural parameters and the position of the components have not been changed. For future configurations, it will be interesting to redesign the blade using the aerodynamic submodule to increase the AEP and doing a structural analysis to redesign the position of the internal components to achieve a configuration more specific for two-bladed turbines.
- Teeter optimization: during this work, a teeter hinge was implemented in the Cp-Lambda model and was subsequently dimensioned manually through a parametric analysis. The goal was to obtain a stiffness that would allow at most a predetermined deflection to guarantee the minimum safety clearance. It would be interesting to implement the design of this component in Cp-Max by inserting the stiffness of the teeter hinge among the global optimization variables.
- Cost model: the teeter hinge implemented into the model is not considered during the evaluation of the costs. The computation of the CoE would be more accurate by adding a cost model for this component. At the moment it has not been implemented because no models have been found in literature.
- Hub, Nacelle, and Tower: due to the introduction of the teeter hinge linked to the hub, the ultimate and fatigue loads have changed on the upper part of the wind turbine and the ground. The elements affected by these load changes are the hub, the nacelle, and the tower. These elements have not been modified from the three-bladed turbine so a redesign of these components could be performed to size them correctly and to reduce the overall costs of the wind turbine.
- Up-wind vs Down-wind: all the configurations considered in this and the previous thesis works at PoliMi concerning the two-bladed turbines are up-wind turbines. It would be interesting to develop a two-bladed down-wind turbine and compare its advantages and disadvantages with a down-wind configuration.
- Cp-Max full optimization: in this work, some analyses have been conducted and a step-by-step structural optimization was performed. This is because leaving the software working on its own using general optimization settings, could lead to obtaining acceptable solutions only after a huge amount of time, since the variables involved are numerous and the path followed might not be the right or the fastest one. However, without the time variable, it would be interesting to perform a complete optimization of the wind turbine using the complete design process of Cp-Max.

Appendix A

Sensitivity Analysis of DLC computational time

During the design process of a wind turbine with the Cp-Max code, a considerable aspect is represented by the computational time necessary for the various phases of the optimizer. The most time consuming sections are the computation of the DLC and the structural optimization process (including fatigue analysis and tip displacement constraint).

In order to reduce the computational time of the DLC, specially for a preliminary design, a sensitivity analysis was carried out to understand if and how it was possible to reduce computation times, affecting the quality of the results as little as possible, through the modification of some settings.

Two of the most representative load cases have been selected for this analysis. The DLC 1.3 at 11m/s 600s long has been selected as the turbulent most difficult condition to deal with, because the wind is an extreme turbulent model and the velocity is close to the rated one. The other DLC selected is the 1.4 v_o and represents an extreme wind change direction at the velocity of cut out, so an extreme condition for loads and for the controller.

The modified variables for this analysis are the integration time-step and the number of FE in which the segments of the blade and of the tower are divided. Considering that computational times depend on the hardware, for this analysis a 4 core CPU has been used with an operative frequency of 3.2GHz.

The reference case has an integration time-step equal to 0.01s, a blade mesh of 60 cubic elements and a tower mesh of 4 cubic elements. These values are taken from a previous setting of the Cp-Max code.

The parameters examined in this analysis come from the force and moment sensors nested in the structure. The relevant parameters analyzed are the flap-wise moment, the edge-wise moment and the torsion, as well as the computational time. It was decided to consider only the blade1 looking at the sensor blade_loads_eta0 that gives results multiplied for a safety factor of 1.35.

In tables A.1 and A.2 there is evidence of the results of the analysis made with some representative combinations of the variables.

	Ref	$\Delta t = 0.02$	FE 20 & 2	FE 25 & 2	FE 30 & 2	FE 30 & 2 $\Delta t = 0.02$
Flapwise [kNm]	191243	191515 (+0,14%)	182681 (-4,48%)	172814 (-9,64%)	179976 (-5,89%)	180181 (-5,78%)
Edgewise [kNm]	86183	86355 (+0,20%)	82109 (-4,73%)	81457 (-5,48%)	83360 (-3,28%)	83584 (-3,02%)
Torsion [kNm]	1354	1327 (-1,93%)	1081 (-25,26%)	1182 (-4,75%)	1289 (-12,61%)	1265 (-6,56%)
CPU time [s]	7653	3898 (-49%)	2723 (-64%)	3218 (-57%)	3686 (-51%)	1803 (-76%)

Table A.1: DLC 1.3 11m/s 600s.

	Reference	$\Delta t = 0.02$	FE 20 & 2	FE 30 & 2	FE 30 & 2 $\Delta t = 0.02$
Flapwise [kNm]	141286	141003 (-0,20%)	135264 (-4,26%)	132928 (-5,92%)	132671 (-6,10%)
Edgewise [kNm]	58638	58618 (-0,03%)	55869 (-4,72%)	56884 (-2,99%)	56865 (-3,02%)
Torsion [kNm]	1260	1261 (-0,01%)	981 (-22,21%)	1215 (-3,65%)	1215 (-3,64%)
CPU time [s]	1201	616 (-49%)	432 (-64%)	583 (-51%)	285 (-76%)

Table A.2: DLC 1.4 vo d.

Through an examination of the results, it can be noticed that by changing only the integration time step the solution remains roughly the same in both DLC with halving the time required. Surely this operation can be also performed for an advanced design and not only for a preliminary one due to the fact that the accuracy is the same.

Another important result is that, as expected, changing the number of FE the solution changes slightly. The model with 20 FE on the blade lost much accuracy in the torsional moment, which is shifted about 20-25%. This might seem a great deal but it must be considered that the torsion is not a dimensioned variable for the structural design in most of the cases, so if the accuracy of this parameter is not required this configuration can be used with 20 FE for a preliminary design. In the other cases the gap with respect to the original configuration is about a few percentage points. At this level of preliminary design this gap is acceptable because it is very close to the original one with the advantage of a significant reduction of computational time.

In the following figures A.1 and A.2 it is possible to view a stretch of the time histories of the two DLC considered. The ranges containing the most critical loads were identified and it is possible to see the trend of the three moments of interest for the all selected configurations.

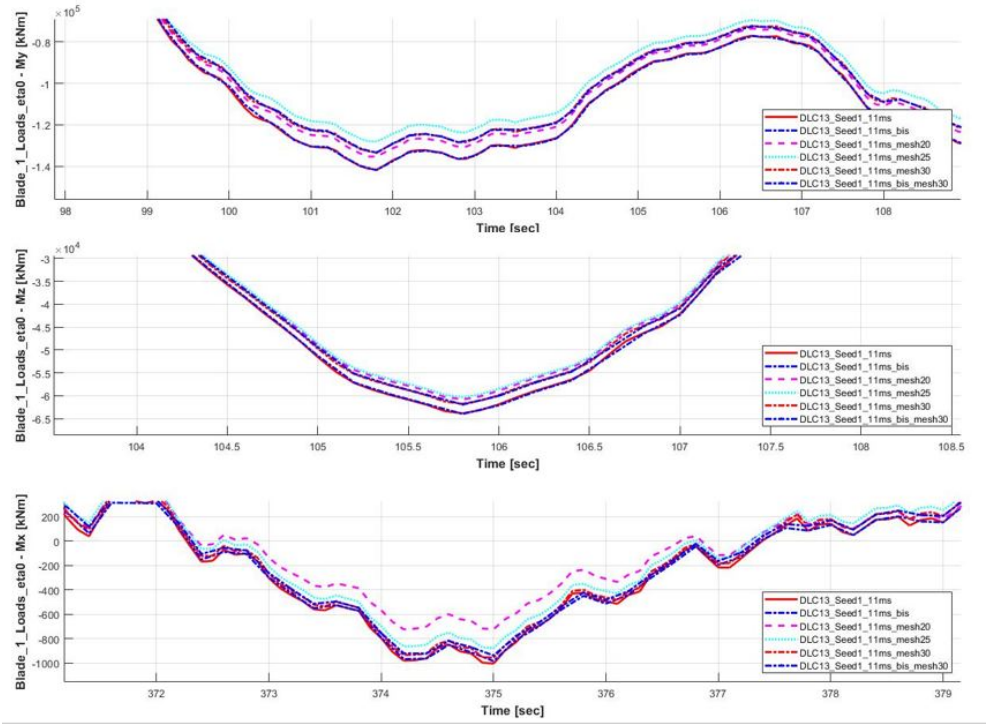

Figure A.1: Loads time history of DLC 1.3 11m/s.

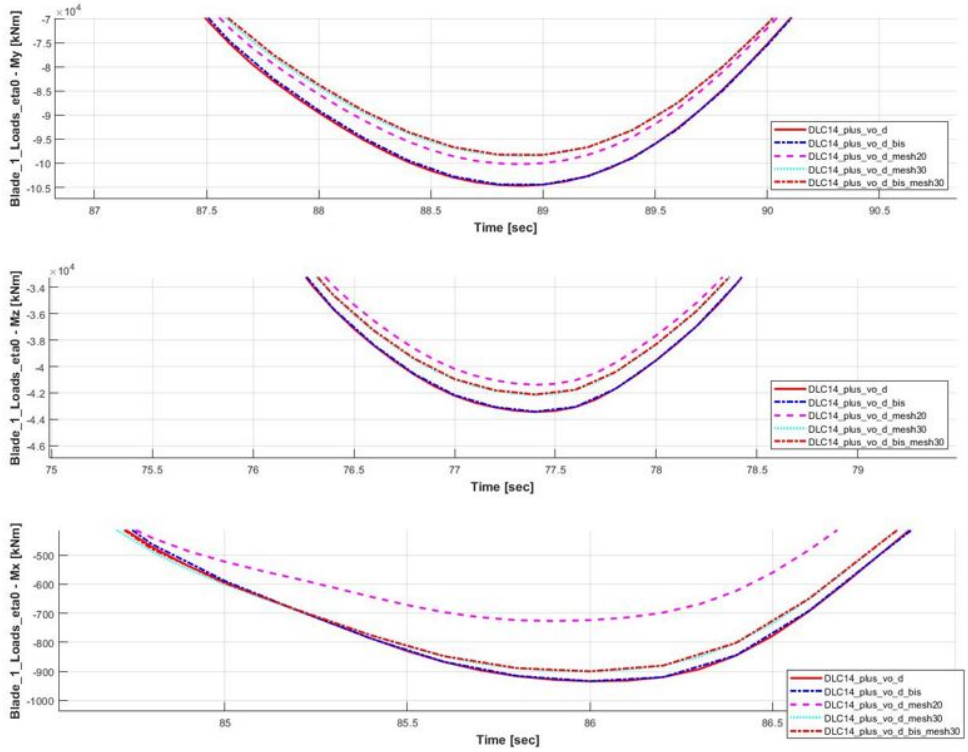

Figure A.2: Loads time history of DLC 1.4 vo d.

An analysis on the combined moment along xy at the base of the tower was also performed to highlight the effect of the variation of the FE number on the tower, and a trend very similar to the original was highlighted for all the cases considered. At this

level of preliminary design, the differences can be negligible, also considering the tower optimization not running. It is possible to view the trend of the analyzed moment in figure A.3 for the different configurations.

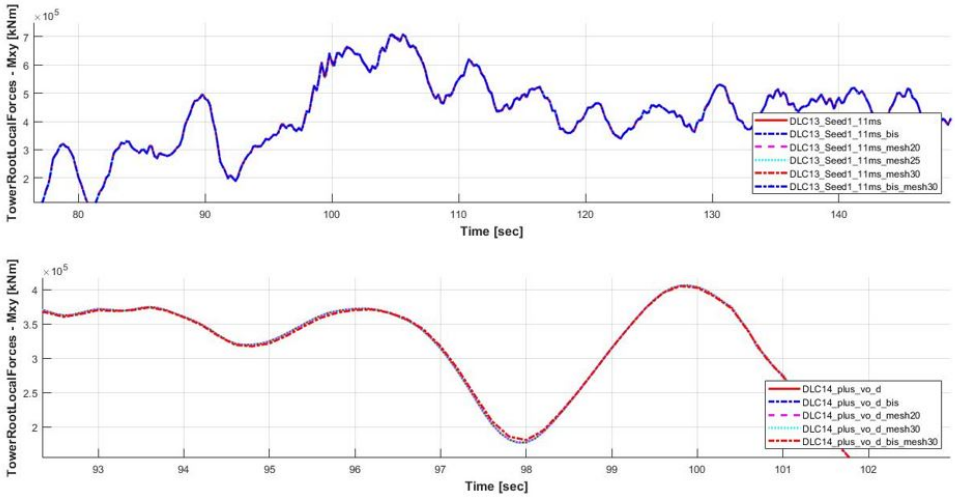

Figure A.3: Loads time history on the tower root.

At the end, the case that combines both modifications, on the integration time step and on the number of FE for the blade model, will be selected. The configuration with 30 FE on the blade and 2 FE on the tower represent a good compromise for a preliminary design, in terms of accuracy and time saving (76%). Considering that about 130 simulations have to be run at each structural optimization loop, it represents a significant saving of time and resources.

Bibliography

[1] F. Anstock, M. Schütt, and V. Schorbach. "A new approach for comparability of two-and three-bladed 20 MW offshore wind turbines." Journal of Physics: Conference Series. Vol. 1356. No. 1. IOP Publishing, 2019.

[2] Ashuri, Turaj, et al. "Aeroservoelastic design definition of a 20 MW common research wind turbine model." Wind Energy 19.11 (2016): 2071-2087.

[3] J. P. Anish. "A comparative analysis of the two-bladed and the three-bladed wind turbine for offshore wind farms". In: (2010).

[4] T. Ashuri, Martins J R R A, Zaaijer M B,van Kuik G A M and van Bussel G J W. 2016 Aeroservoelastic design definition of a 20 MW common research wind turbine model Wind Energy 19 2071–2087 https://onlinelibrary.wiley.com/doi/abs/10.1002/we.1970.

[5] F. Bellini. "Preliminary design of a 20 MW wind turbine". Master thesis. Politecnico di Milano, July 27, 2017.

[6] K. Boorsma et Al 2016 INNWIND Deliverable 2.14 New aero-structure rotor concepts and evaluation for 20 MW turbines INNWIND.EU December 2016.

[7] E. A. Bossanyi, P. A. Fleming, and A. D. Wright. "Validation of individual pitch control by field tests on two-and three-bladed wind turbines". In: IEEE Transactions on Control Systems Technology 21.4 (2013).

[8] C. L. Bottasso - F. Campagnolo - A. Croce, Multi-disciplinary constrained optimization of wind turbines. Multibody System Dynamics, 27: 21-53, 2011, ISSN: 1384-5640, DOI: https://doi.org/10.1007/s11044-011-9271-x.

[9] C. L. Bottasso - A. Croce, Cp-Lambda a Code for Performance, Loads, Aeroelasticity by Multi-Body Dynamics Analyisis. Ver. 5.20, Politecnico di Milano, June, 2010.

[10] C. L. Bottasso, F. Campagnolo, and A. Croce. "Multi-disciplinary constrained optimization of wind turbines". In: Multibody System Dynamics 27.1 (Jan. 2012), pp. 21–53. ISSN: 1573-272X. DOI: 10.1007/s11044-011-9271-x.

[11] T. Burton et al. Wind energy handbook. John Wiley & Sons, 2011.

[12] P. Chaviaropoulos et Al 2017 INNWIND Deliverable 1.25 PI-based assessment (application) on the results of WP2-WP4 for 20 MW wind turbines INNWIND.EU September 2017.

[13] M. Civati. "Design of a Two-Bladed 10MW Wind Turbine with Teetering Hub". Master thesis. Politecnico di Milano, 2017.

[14] A. Croce, Poli-Wind research, dispensa del corso "Progetto di generatori eolici", 2019.

[15] J. Dai, X. Yang, L. Wen, Development of wind power industry in China: A comprehensive assessment, Renewable and Sustainable Energy Reviews, Volume 97, 2018, ISSN 1364-0321, https://doi.org/10.1016/j.rser.2018.08.044.

[16] M. Diaz & R. Cardenas & M. Espinoza & A. Mora & F. Rojas, (2015). A Novel LVRT Control Strategy for Modular Multilevel Matrix Converter based High-Power Wind Energy Conversion Systems. 10.1109/EVER.2015.7113026.

[17] P. Dvorak, The plus side of large two-blade turbines, May 6, 2010, Sweeden, windpowerengineering.com.

[18] L. Fingersh - M. Hand - A. Laxson, Wind Turbine Design Cost and Scaling Model. Technical Report, NREL/TP-500-40566, December, 2006, https://doi.org/10.2172/897434.

[19] V. Giavotto, M. Borri, P. Mantegazza, G. Ghiringhelli, V. Carmaschi, G. C. Maffioli, and F. Mussi. "Anisotropic beam theory and applications". In: Computers & Structures 16.1 (1983), pp. 403–413. ISSN: 0045-7949. DOI: https://doi.org/10.1016/0045-7949(83)90179-7

[20] G. Giulianini, Design of a 20 MW two-bladed wind turbine. Master thesis. Politecnico di Milano, 2020.

[21] "Guideline for the Certification of Wind Turbines". Hamburg: Germanischer Lloyd Industrial Services GmbH. 2010.

[22] INNWIND.EU Deliverable 1.23, PI-based assessment of innovative concepts (methodology). INNWIND.EU technical report, Deliverable 1.23, DOI: https://www.innwind.eu, April 2014.

[23] International Electrotechnical Commission. IEC 61400-1 Wind Turbines - Part 1: Design Requirements, 3rd Edition, 2006.

[24] B.J. Jonkman and L. Kilcher. TurbSim User's Guide: Version 1.06.00. NREL Technical Report, September 2012.

[25] J. F. Manwell - J. G. McGowan - A. L. Rogers, Wind Energy Explained: Theory, Design and Application. 2nd Edition, John Wiley & Sons, 2009.

[26] R. Nijssen et Al 2016 INNWIND Deliverable 4.15 Innovations on component level for coming 20MW turbines (final report) INNWIND.EU September 2016.

[27] J. Peeringa, R. Brood, O. Ceyhan, W. Engels and de G. Winkel. 2011 Upwind 20MW Wind Turbine Pre-Design Report ECN-E–11-017, Energy Research Center of the Netherlands.

[28] J. Peeringa, R. Brood, O. Ceyhan, W. Engels, and G. De Winkel, Upwind 20 MW wind turbine pre-design. Petten: ECN, 2011.

[29] S. Pontow , D. Kaufer, Shirzahdeh and K¨uhn M 2017 INNWIND Deliverable 4.36 Design Solution for a Structure Concept for future 20MW INNWIND.EU September 2017.

[30] P. C. Putnam, Putnam's Power from the Wind. G W Koeppl, New York (NY), USA, 1982.

[31] L. Sartori et al. "Preliminary design and optimization of a 20MW reference wind turbine." Journal of Physics: Conference Series. Vol. 1037. No. 4. IOP Publishing, 2018.

[32] L. Sartori. "System design of lightweight wind turbine rotors". PhD thesis. Politec-

nico di Milano, 2019. DOI: http://hdl.handle.net/10589/144667

[33] L. Sartori, P. Bortolotti, A. Croce, C.L. Bottasso, Integration of prebend optimization in a holistic wind turbine design tool. TORQUE, Munich, Germany, 5-7 October, 2016.

[34] V. Schorbach, P. Dalhoff, and P. Gust, "Teeter design for lowest extreme loads during end impacts," Wind Energy, vol. 21, no. 1, Art. no. 1, 2018.

[35] V. Schorbach - P. Dalhoff, Two bladed wind turbines: antiquated or supposed to be resurrected? Proceedings of EWEA 2012, European Wind Energy Association (EWEA), Copenhagen, Denmark, April, 2012.

[36] "Seawind's innovative high-performing turbine". DOI: https://seawindtechnology.com/solutions/. Accessed March 2021.

[37] Vergent Eolien, DOI:http://www.vergnet.com/. Accessed March 2021.

[38] Wind Turbine Models. DOI: https://en.wind-turbine-models.com/. Accessed March 2021.